A final report to the Chesapeake Bay Trust
108 Severn Ave, Annapolis, MD 21403

A SHELL BUDGET FOR THE CHESAPEAKE BAY OYSTER RESOURCE.

Lead investigator: Roger Mann
address: Virginia Institute of Marine Science, Gloucester Point VA 23062.
e-mail: rmann@vims.edu
phone: 804-684-7360 (office) , 804-815-3550 (cell)

Collaborating investigators:
Melissa Southworth
address: Virginia Institute of Marine Science, Gloucester Point VA 23062.
e-mail: melsouth@vims.edu
phone: 804-684-7821 (office)

James Wesson (retired VMRC)
formerly: Virginia Marines Resources Commission, Newport News VA
e-mail: jw12050@aol.com

John Thomas
address: Virginia Institute of Marine Science, Gloucester Point VA 23062.
e-mail: jkthomas@vims.edu
phone: 804-684-7183 (office)

Mitch Tarnowski
address: Maryland Department of Natural Resources, 580 Taylor Ave., B-2, Annapolis, Maryland 21401
e-mail: mitch.tarnowski@maryland.gov
410-260-8258 (office)

Mark Homer (deceased, formerly MD DNR)

Date of submission: July 10, 2019

Extant reefs are losing the race with sea level rise and sedimentation; reefs represented in the fossil record had the race in hand. The disparity between the two is stark and unlikely to be reduced given the inability of oysters to survive to older ages in the current Bay ecosystem. This opinion is strongly supported by the current analysis. There is a fundamental challenge with longevity for Bay oysters and it cannot be blamed entirely on harvest or disease. A broader consideration of the Bay watershed and its input to the Bay should be carefully scrutinized. Truncated population structure reduces input of shell to the underlying reef structure such that the latter is not sustainable without continual shell repletion. Restoration to self-sustaining reef structures is unlikely, if not impossible, in extant oyster populations in the Bay.

Table of contents

#2 is a three part mortality protocol with M1 (0-2y) of 0.55, M2 (3-11 y) increasing from 0.05 to 0.12, and M4 (12-20y) of 0.4. The fossil growth curve of Lockwood and Mann is employed. Label 1 through 8 of sequence #1 correspond to 1 through 8 in Figure 19. Sequence #1 is a three part mortality protocol with M1 (0-2y) of 0.55, M2 (3-8 y) increasing from 0.05 to 0.12, and M4 (9-20y) of 0.4. The fossil growth curve of Lockwood and Mann is employed. Label 1 through 8 of sequence 1 correspond to 1 through 8 in Figure 19. The data of Figure 14 of this report is include for comparison purposes. A single value of M is employed for the 0-9 y period, with M increasing sequentially from 0.58-0.72. The composite MD age at length curve (see page 21) is employed. See text for additional discussion of Filtration Index.

Figures:

Figure 1: scenarios "Base case" and options #1 through #6. Graphical descriptions of shell pools and processes connecting them in terms of both addition process (in blue) and loss processes (in red). Graphics modified from Chesapeake Bay GIT presentation on March 27, 2017. See text for additional details.

Figure 2: An illustration of the influence of shell allometry on shell mass and contributions of year class structure to overall shell budgets.

Figure 3. Aggregation of sampling area in the Virginia Chesapeake Bay. See text for additional details.

Figure 4. MD data, all reefs, 2010-2015 shell length frequency by 2mm intervals with a 6mm smoothing.

Figure 5. An illustration of year class identification in MD data using TropFish R. See text for additional details.

Figure 6. Time series demographic of oyster in the Piankatank River. Blue is YOY, all other year classes in red. See text for additional details.

Figure 7. Piankatank River oysters, 2006-2016. Age at length, percentage survival (1-mortality), and shell length versus dry meat (SL v DMW) and shell length versus dry shell weights (SL v DSW).

Figure 8: Piankatank River oysters: shell weight demographic for 2006-2016. See text for additional details.

Figure 9A. Piankatank River: partitioning of shell volume (in bushels) 2006-2016 as live shell, brown (oxic) and black (anoxic) shell layers, plus a total value.

Figure 9B. Virginia Chesapeake Bay: partitioning of shell volume (in bushels) 2006-2016 as live shell, brown (oxic) and black (anoxic) shell layers, plus a total value

Figure 10. Virginia Chesapeake Bay, 2006-2016: Time series observations of brown shell volume (L m^{-2}) versus live shell volume (L m^{-2}).

Figure 11. Demographic profile of shell weight per unit area on MD reefs by year class for year classes originating in 2006 through 2015. Note that the plot ordinates have a variety of scales to accommodate spatial differences. The color sequences on the plots are standard across all plots; for example the 2012 year class for MD is mid green for all sites. MD reef labels are given in the accompanying text.

Figure 12. Demographic profile of shell weight per unit area on VA reefs by both year and year class for year classes originating in 2006 through 2016. Note that the plot ordinates have a variety of scales to accommodate spatial differences. The color sequences on the plots are standard across all plots; for example the 2009 year class for VA is orange for all sites.

Figure 13. Allometric relationships of SL (mm) v DSW (g): Left panel -MD data for 2011-2013 by individual sites as described in Table 4. Mid panel - VA data for 2006-2010 with all sites combined (the highlighted yellow values in Tables 5-7), and 2010 VA data for James River (Table 6). All plots are SL truncated between 30 and 140 mm SL on x axis, versus DSW in gm on the y axis.

Figure 14. Simulations based on Figures 11 and 12. A: survival as a declining function wherein annual mortality, M, is a proportional value between 0.0 (no mortality) and 1.0 (all died). M values are consistent color coded among panels between 0.58 and 0.72. Survival is (1-M). B: standing stock of shell (g m^{-2}). C: annual shell Production (g $m^{-2}y^{-1}$). D: annual shell Loss (g $m^{-2}y^{-1}$). See text for additional details.

Figure 15. Figure 1 of Lockwood and Mann (2019, in review). Length frequency *(a)* and age at length *(b)* of Pleistocene oyster shells from the Piankatank River VA and modern shells from the James River VA.

Figure 16. Length at age for fossil oyster shells: combined data from Piankatank River collection (blue, from Lockwood and Mann in Figure 15) and offshore New York (orange). See text for additional details.

Figure 17. A proposed revision of Figure 5 from Walles et al (2015). The original Weibull distribution fit ($\lambda = 1$, $\kappa = 0.6$) is the solid line fitted to survivorship data (mean + s.e.) of three oyster populations (Viane, St. Annaland and Kats) in the Oosterschelde estuary, Netherlands (raw data in Figure 18). The proposed revision of the mortality curve is the broken line and incorporates three distinct mortality rates over the life expectancy.

Figure 18. Length frequency distribution of oysters, *Crassostrea gigas* , pooled in 5 mm sizes bins, collected in 0.25 m^2 quadrants (n = 10) on three intertidal oyster reefs in the Oosterschelde estuary (The Netherlands): Viane, sampled November 1st 2011 (n = 2640); St. Annaland, sampled February 9th 2012 (n = 1341); Kats, sampled February 7th 2012 (n = 990). Year classes are separated by dashed lines. The arrows indicate the mean shell length for each year class. Source: Walles et al (2015)

Figure 19. Time series of survival, live shell standing stock (g m^{-2}), shell production and shell loss (g m^{-2} y^{-1}) for an oyster population with an initial density of 100 m^{-2} with varying sequences of mortality over a 20 year period. Sequence #1 is a three part mortality protocol with M1 (0-2y) of 0.35, M2 (3-11 y) increasing from 0.05 to 0.12, and M4 (12-20y) of 0.4. The fossil age at length curve of Figure 1B of Lockwood and Mann (see Figure 15 of this report) is employed. Label 1 through 8 of plots describing live shell weight, shell production and shell loss correspond to mortality rate sequences in the footer of the top panels of each sequence. See Table 9 and text for additional details.

Figure 20. Cumulative fecundity (all size classes, egg m-2 y-1) for VA regions by year. All plots have the same axes with shell length on x axis and fecundity on ordinate. Note that ordinates are area specific in scale. All panels have the same color coding for years (e.g., 2009 is yellow throughout).

Introduction.

Oysters, *Crassostrea virginica*, are unusual in that they are both critical live organisms in temperate to tropical coastal and estuarine food webs, and critical components of the physical habitat (hard substrate) and chemical (carbonate and alkalinity) budgets in those same environments. Management of oysters requires consideration of two biological reference points, one for the live oysters and one for the shell that results from their death (Powell and Klinck 2007, Mann and Powell 2007, Mann et al 2009b, Harding et al 2010, Southworth et al 2010). These are not the same, and a general consideration of (1) the evolution of oysters and (2) the time course of oyster reef formation with rise and fall of sea level over recent geological time indicates that much of the shell accumulation from natural mortality of oysters is required to maintain, and indeed build reef structures. The "shell budget" has generally been ignored over the history of oyster fisheries as demonstrated by the historical overfishing and decimation of reef associated oyster resources on a global basis. We in the Chesapeake Bay are not alone in failing to apply sensible proactive quantitative management of the reef resource. The emergence of the arguments proffered by Powell and Klinck (2007), Mann and Powell (2007) and others has stimulated greater interest in preservation and rebuilding of oyster resources with equal inclusion of management of the shell resource. Thus a need is evident for a current consideration of the status of both oyster and oyster shell resources in the Chesapeake Bay.

The Chesapeake Bay Trust approached the lead investigator to develop a shell budget for the Chesapeake Bay oyster resource. I begin this report with a combination of text description and a series of graphics that explain the underlying approach to developing a shell budget. This description is built on the following:

1. In BOTH restoration efforts and fishery management efforts there must be a goal of ***No Net Loss of living oysters or shell substrate***.
2. Oyster recruitment (R) and growth dictate addition to the living component of a reef.
3. Natural mortality (M) and fishing mortality (F) both dictate loss of live oysters.
4. M contributes to the shell substrate on the underlying reef, F does not because oysters are removed.
5. High mortality (M) rates result in low shell accumulation because contributing oysters are small – low mortality rates are preferable because oysters survive to larger size and contribute much more shell when they die.
6. Shell on the reef is lost to burial (B) and biological and chemical degradation (D).
7. Shell loss rates are probably salinity dependent and independent of supply from mortality.
8. Stable reefs require equilibrium between shell addition and loss, and therefore requires sustained recruitment, growth and survival of oysters to large size prior to death. Accreting reefs require shell addition to exceed loss.
9. Offsetting inadequate shell supply from mortality (M) through repletion (r) is NOT a single addition process – it requires continuing addition forever.
10. Single replenishment action to suitable bottom IS NOT restoration.

Developing a shell budget: a step by step protocol.

Herein I describe the general step-wise process of developing a shell budget from a stock assessment data set, and subsequently the spatially specific shell budget for the composite areas of the Chesapeake Bay.

The stock assessment source database from both MD and VA provides a multi-year monitoring of oyster density (numbers per unit area) and shell density (weight or volume per unit area) by reef. Additional details of these surveys, including their strengths and weakness for the purpose of this report, are addressed later in the text. The live oyster data generates values for both numbers of oysters m^{-2}, and the demographic of those oysters by length (SL, longest dimension from the hinge to the growing edge in mm, this should correctly termed shell height but I adopt the commonly accepted convention of length for this report) intervals at the mm or 2mm size interval level for both VA data and MD data. From subsamples of the

oysters the length demographic can be converted by equations describing (1) length versus biomass as whole live weight (SL(mm) v LW(g)), (2) length versus biomass as dry meat weight (SL(mm) v DW(g)), (3) length versus dry shell weight ((SL(mm) v SW(g)), and (4) length versus wet shell weight ((SL(mm) v WSW(g)) to other spatially descriptive values. Thus, the standing stock can be described as not just as numbers oysters m^{-2} but also live biomass m^{-2} inclusive of shell, dry tissue weight m^{-2}, dry shell weight $m^{-2,}$ and wet shell weight m^{-2}. Note that these are live standing stock values. I will address the shell substrate values shortly. What we desire is rates of live oyster production and loss, and for this we use a time series of annual assessment standing stock values from both states in concert with growth and mortality rates.

How do we estimate the values of growth and mortality? Consider a time series of demographic data. Demographic analysis identifies cohorts. If these are annual then the chosen demographic provides a description of year class structure. Now consider a sequence of demographics of year class structure and the inter-annual change in any of the above descriptors provides both a mortality and a production estimate for a chosen year class as it is followed over time. Consider Table 1 as a matrix of 5 demographics each representing one year of observations. Each year has a total number of oysters m^{-2} and the sub division of that total into 4-year classes where year class 0 is the young of the year (YOY = new recruits).

Table 1. Example oyster demographics by number m^{-2}

	Total # oysters m^{-2}	Year class			
		0	1	2	3
year of observation					
1	100	60	25	10	5
2	150	100	30	15	5
3	120	60	40	15	5
4	160	110	30	15	5
5	200	130	50	15	5

It is possible to follow the progression of one year of recruits through time. The YOY (year class 0) from year 1 has 60 oysters m^{-2} in that year, 30 oysters m^{-2} in year 1, 15 oysters m^{-2} in year 2 and 5 oysters m^{-2} in year 3. **Sequential mortality** is this ((60-30)/60) from year 0 to year 1, ((30-15)/30) from year 1 to year 2, and ((15-5)/5) from year 2 to year 3. These estimates are mortality as a proportion of the live oysters at the beginning of the year. They can easily be expressed as percentages. Estimating cumulative rather than inter annual, age specific mortality requires only a minor modification to these expressions.

Table 2. Example oyster demographics by biomass m^{-2}

		Year class			
		0	1	2	3
	mean DW for year class	a	b	c	d
	Total # oysters m^{-2}	DW by year class			
year of observation					
1	100	60a	25b	10c	5d
2	150	100a	30b	15c	5d
3	120	60a	40b	15c	5d
4	160	110a	30b	15c	5d
5	200	130a	50b	15c	5d

If we know mean SL for each year class then we can estimate biomass as, for example DW as described earlier for each year class and thus modify Table 1 to describe dry meat biomass in each year class for each

year of observation. This is illustrated in Table 2 where DW in each year class is (# oysters m^{-2} x mean DW) for the oyster in that size class. The sum of the dry meat biomass of each year class in each sequential year describes how biomass per unit area fluctuates from year to year. Dry meat production can be described in a manner similar to that of mortality. For example, production of the YOY year class in the year 1 to year interval is (30b – 60a) in absolute units, or ((30b – 60a)/60a) as a proportion and so on.

To progress from dry meat to shell production we can again modify the table. There is generally a strong relationship between shell dry weight and dry meat biomass in oysters (the condition index). For the sake of simplicity let us assume that within any size or age class that dry shell weight, SW, is a constant 10X the dry meat weight value - it may vary and this can be evaluated as part of monitoring, but I assume a constant here to keep the explanation simple. Variation in size versus biomass or shell is addressed in detail later in this report as a discussion of variation in allometric descriptors of both for various locations (MD data) or aggregations of locations (VA data). The above Table 2 is again modified thus to produce Table 3:

Table 3. Example oyster demographics by dry shell weight m^{-2}

		Year class			
		0	1	2	3
	mean SW for year class	10a	10b	10c	10d
	Total # oysters m^{-2}	SW by year class			
year of observation					
1	100	600a	250b	100c	50d
2	150	1000a	300b	150c	50d
3	120	600a	400b	150c	50d
4	160	1100a	300b	150c	50d
5	200	1300a	500b	150c	50d

Calculating total SW m^{-2} by sequential year illustrates how the standing SW as live oysters fluctuates. Thus, the values for years of observation 1 through 5 are (600a + 250b + 100c + 50d) for year class 1 and so forth. Again, this is the LIVING component of the standing shell stock per unit area. Now we can estimate how, with mortality, shell is added to the inanimate shell pool that forms part of the reef structure/habitat. Thus, in transition from year 1 to year 2 in Table 3 above 30 individuals survive from YOY to year class one status and the associated shell biomass has changed from 600a to 300b units, but 30 individuals from that year class have also died and have contributed their shells to the underlying reef. The challenge in estimating the shell contribution is the unknown point in time when the mortality occurred. If mortality occurred on the day after sampling in year 1 then the shell addition is 300a units. If, on the other hand the mortality occurred on the day before sampling in year 2 the shell addition is 300b units. By progressing these calculations across the time frame in Table 3 we estimate the total of both live shell production and that newly added to the underlying reef by mortality. The process can be repeated for wet shell weight and so on.

If the above described situation persisted there would be a continuous accumulation of shell. This is not the case. Shells is lost to burial, mechanical disintegration, and dissolution. The last two listed can be facilitated by biological action such as boring. These loss processes in aggregation are termed taphonomic processes. Importantly, taphonomic processes continue independent of processes that produce shell and add it to the underlying reef structure. Long term taphonomic loss continues in the absence of oyster recruitment, growth and mortality, and can result in irretrievable loss of reef structure. The survey database in VA includes standing estimates of shell volume in units of L m^{-2} as both brown shell (volume above the sediment water interface in oxic water) and black shell (volume below the sediment water interface in anoxic sediment). The survey database in MD focuses on brown shell. Taphonomic loss is estimated as the

difference between estimated cumulative shell (from Table 3 above for dry shell or a similar construct for wet shell) and observed shell volume in the survey database. Note there is a change in units herein – production is estimated in weight whereas shell presence is in volume. This is an historic artifact in that these parameters were set in place prior to any construct for developing fine estimates of shell budgets. Shell planting and management was and is in volumetric units – bushels. Just to be cantankerous the MD bushel at 45.9L differs from the VA bushel at 50L. The implementation of a weight to volume conversion function was and is simple and is described in Mann et al (2009a, 2009b).

Now we have all the parts on an annual basis – shell in live oysters, brown shell and black shell in units of L. Progress from one year to the next and include the production of new live shell and transfer of shell to the inanimate pool through mortality. The difference between the estimated sum and the measured sum is that lost to taphonomy. Thus we have a loss rate that can be expressed as an absolute rate per unit area, a rate related to standing stock and/or production of live oysters on that unit area (so providing stock and production rate estimates that are required to balance loss and retain environmental integrity), a rate related to local environmental conditions of salinity, turbidity, food and/or other considerations, and more as desired. What is obvious from this discussion is that estimation of shell production is not a constant rate for all situations, and its balance against loss will vary between locations and over time. The long-term goal must not be equilibrium, it must be that of accretion where addition of shell to the underlying reef through mortality exceeds loss to taphonomy in order to insure reef accretion. This is how reefs grow over geological time with sea level rise, and how we should set targets for both restoration and fishery. For restoration activity we desire that reefs continue to accrete after we have implemented restoration – we cannot, and this is very important, rely on continual repletion to maintain the reef structure. For fishery management we desire to limit exploitation so that underlying reef structure is not degraded over continuing time. Finally, the series of estimations outlined above is only as good as the data contributing to the estimations. In truth neither the MD nor VA surveys were originally designed with shell budget estimation in mind. The data can be used in part for this purpose, and in describing my estimations I will highlight the limitations of the data where they arise.

A graphical depiction of options.

The above following description was presented to the Chesapeake Bay GIT on March 27, 2017 as a PowerPoint presentation. That file has been restructured below and starts with a base case relationship between oyster demographics, recruitment and mortality rates, and taphonomy. Six additional cases (scenarios #1 through 6) selectively include or not replenishment and fishing. The important summary for each of the 6 numbered scenarios is in the top left box in each graphic. Only a limited number of scenarios are stable over time, that is not requiring of continual shell replenishment.

Figure 1: scenarios "Base case" and options #1 through #6. Graphical descriptions of shell pools and processes connecting them in terms of both addition process (in blue) and loss processes (in red). Graphics modified from Chesapeake Bay GIT presentation on March 27, 2017. See text for additional details.

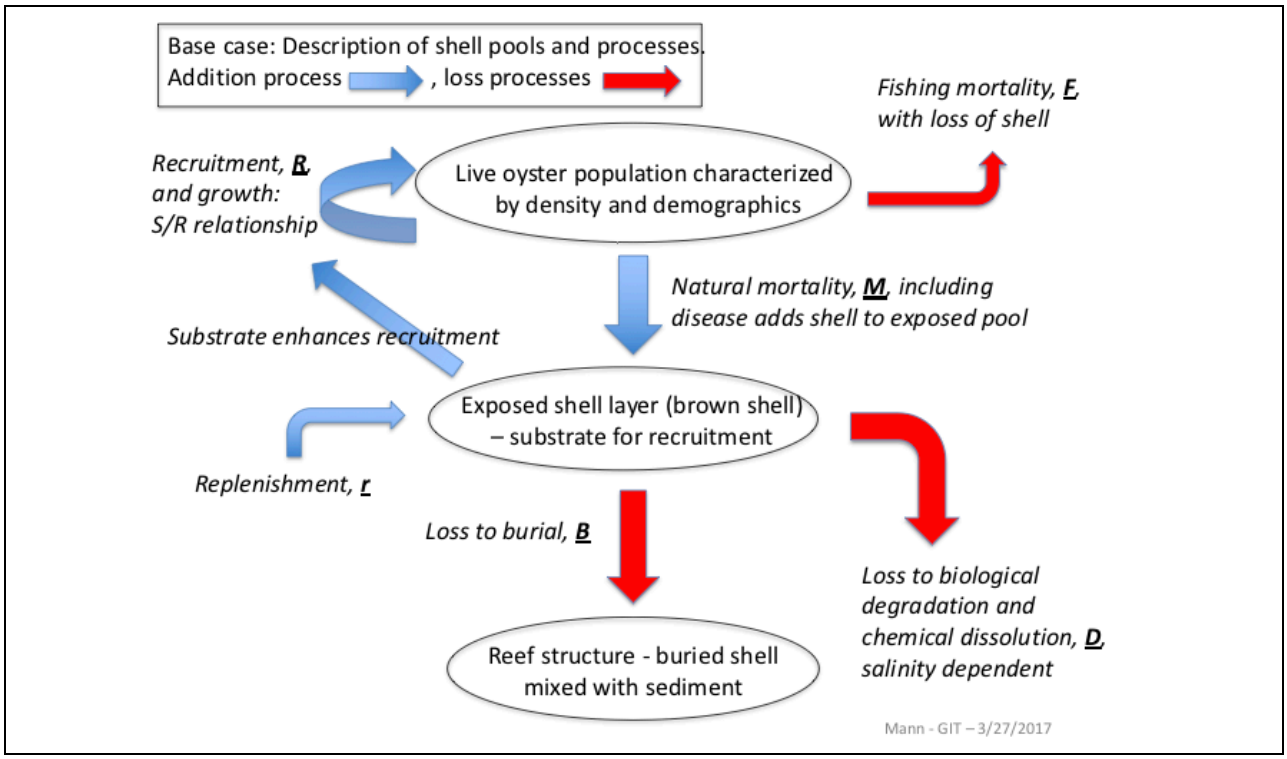
Base case: Description of shell pools and processes.
Addition process , loss processes
Fishing mortality, F, with loss of shell
Recruitment, R, and growth: S/R relationship
Live oyster population characterized by density and demographics
Natural mortality, M, including disease adds shell to exposed pool
Substrate enhances recruitment
Exposed shell layer (brown shell) – substrate for recruitment
Replenishment, r
Loss to burial, B
Loss to biological degradation and chemical dissolution, D, salinity dependent
Reef structure - buried shell mixed with sediment
Mann - GIT – 3/27/2017

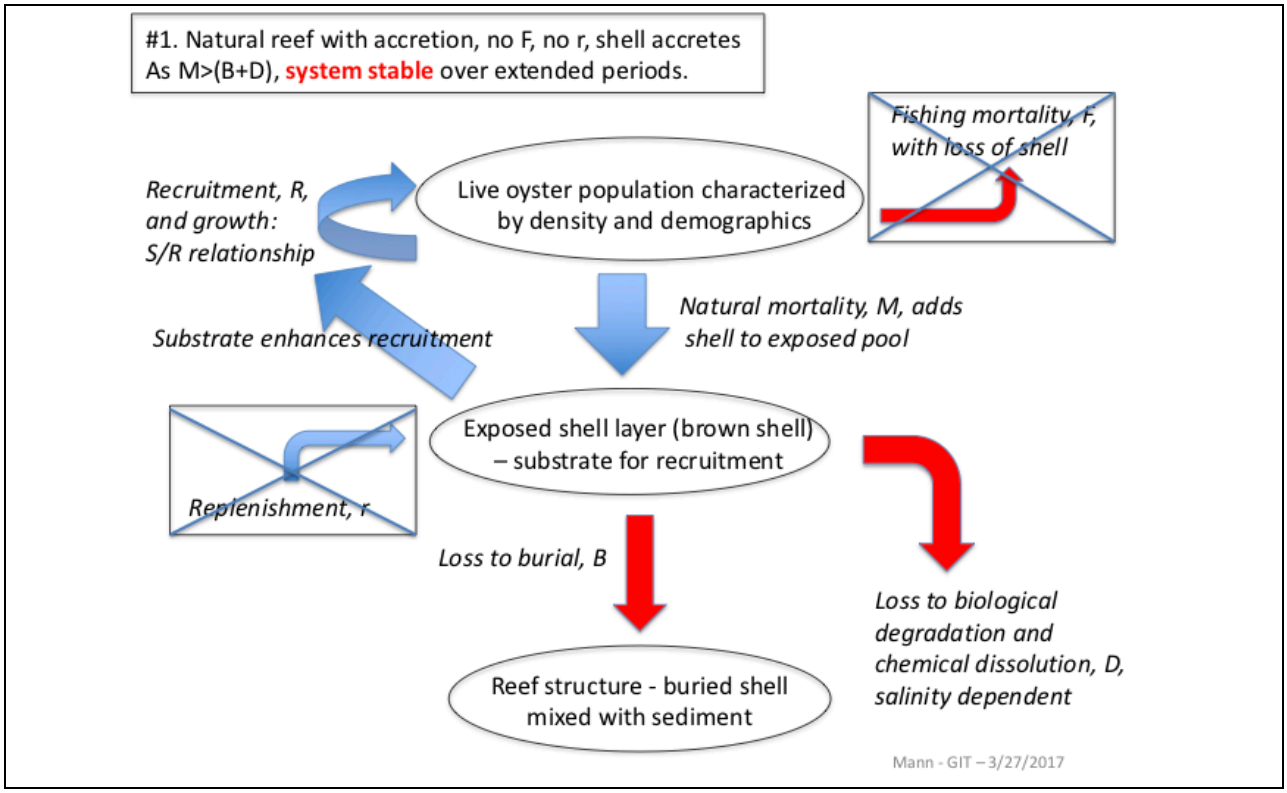
#1. Natural reef with accretion, no F, no r, shell accretes
As M>(B+D), system stable over extended periods.
Fishing mortality, F, with loss of shell
Recruitment, R, and growth: S/R relationship
Live oyster population characterized by density and demographics
Natural mortality, M, adds shell to exposed pool
Substrate enhances recruitment
Exposed shell layer (brown shell) – substrate for recruitment
Replenishment, r
Loss to burial, B
Loss to biological degradation and chemical dissolution, D, salinity dependent
Reef structure - buried shell mixed with sediment
Mann - GIT – 3/27/2017

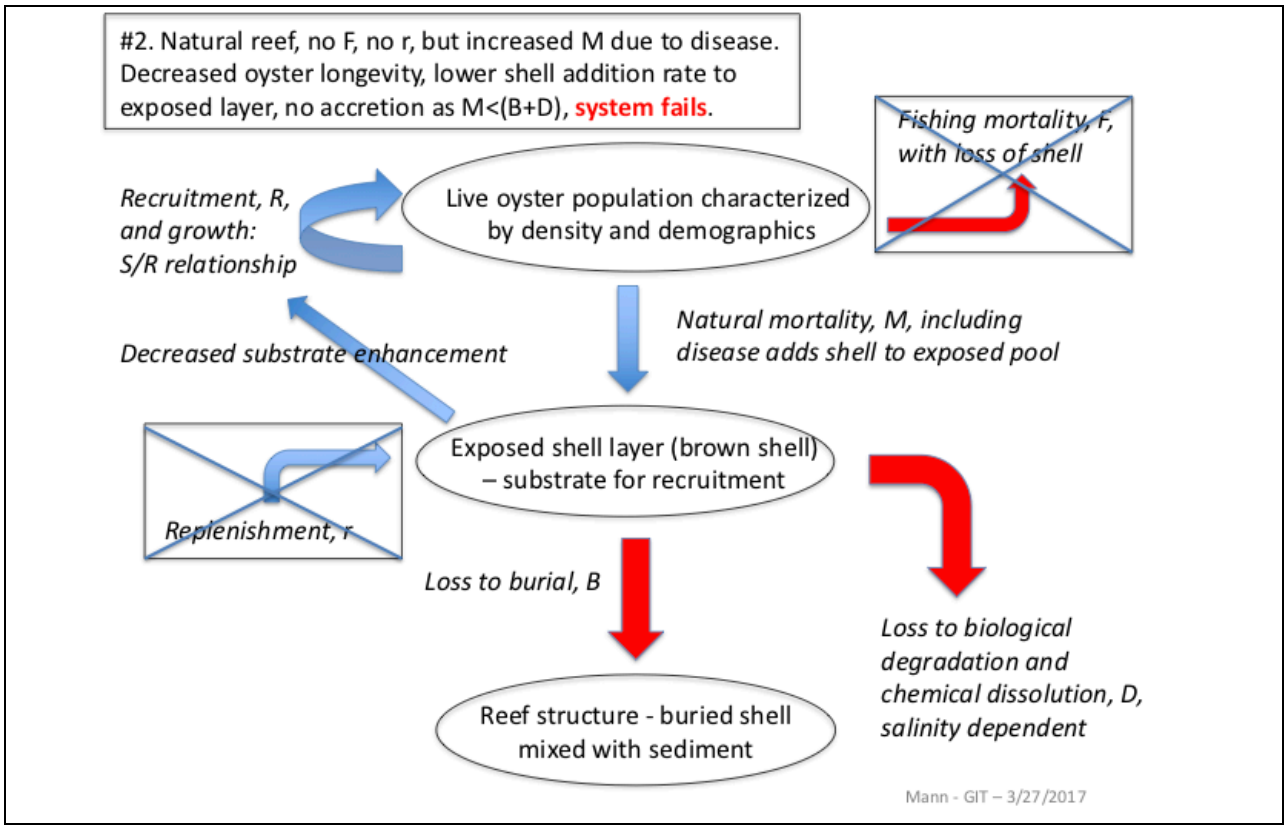
#2. Natural reef, no F, no r, but increased M due to disease. Decreased oyster longevity, lower shell addition rate to exposed layer, no accretion as M<(B+D), system fails.
Fishing mortality, F, with loss of shell
Recruitment, R, and growth: S/R relationship
Live oyster population characterized by density and demographics
Natural mortality, M, including disease adds shell to exposed pool
Decreased substrate enhancement
Exposed shell layer (brown shell) – substrate for recruitment
Replenishment, r
Loss to burial, B
Loss to biological degradation and chemical dissolution, D, salinity dependent
Reef structure - buried shell mixed with sediment
Mann - GIT – 3/27/2017

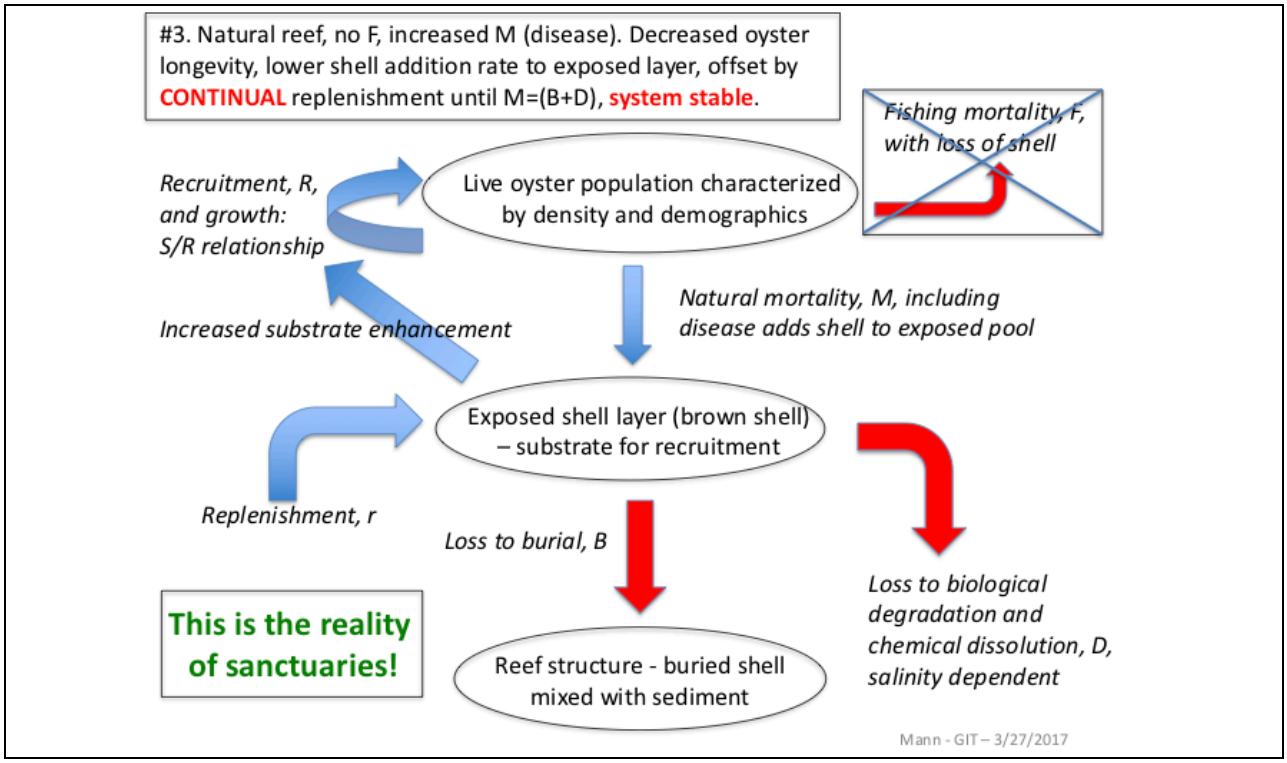
#3. Natural reef, no F, increased M (disease). Decreased oyster longevity, lower shell addition rate to exposed layer, offset by CONTINUAL replenishment until M=(B+D), system stable.
Fishing mortality, F, with loss of shell
Recruitment, R, and growth: S/R relationship
Live oyster population characterized by density and demographics
Natural mortality, M, including disease adds shell to exposed pool
Increased substrate enhancement
Exposed shell layer (brown shell) – substrate for recruitment
Replenishment, r
Loss to burial, B
This is the reality of sanctuaries!
Loss to biological degradation and chemical dissolution, D, salinity dependent
Reef structure - buried shell mixed with sediment
Mann - GIT – 3/27/2017

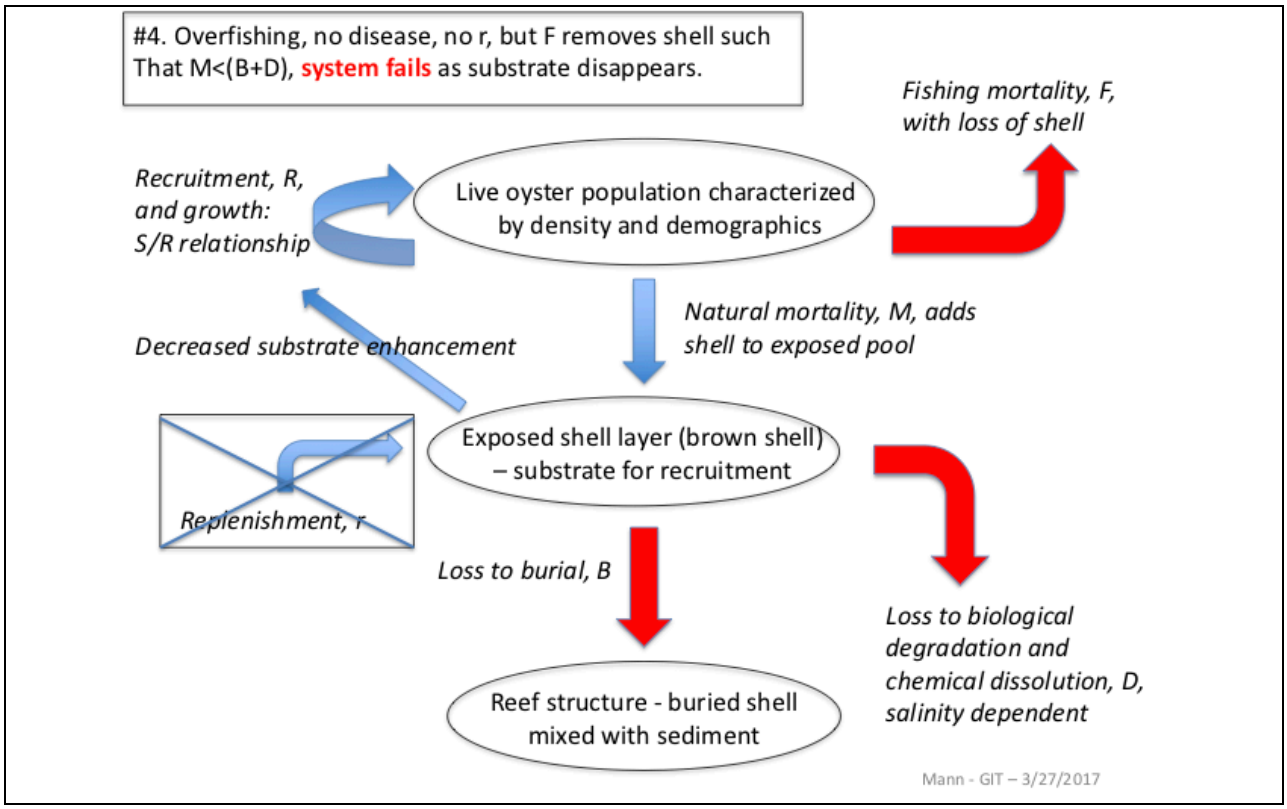
#4. Overfishing, no disease, no r, but F removes shell such That M<(B+D), system fails as substrate disappears.
Fishing mortality, F, with loss of shell
Recruitment, R, and growth: S/R relationship
Live oyster population characterized by density and demographics
Natural mortality, M, adds shell to exposed pool
Decreased substrate enhancement
Exposed shell layer (brown shell) – substrate for recruitment
Replenishment, r
Loss to burial, B
Loss to biological degradation and chemical dissolution, D, salinity dependent
Reef structure - buried shell mixed with sediment
Mann - GIT – 3/27/2017

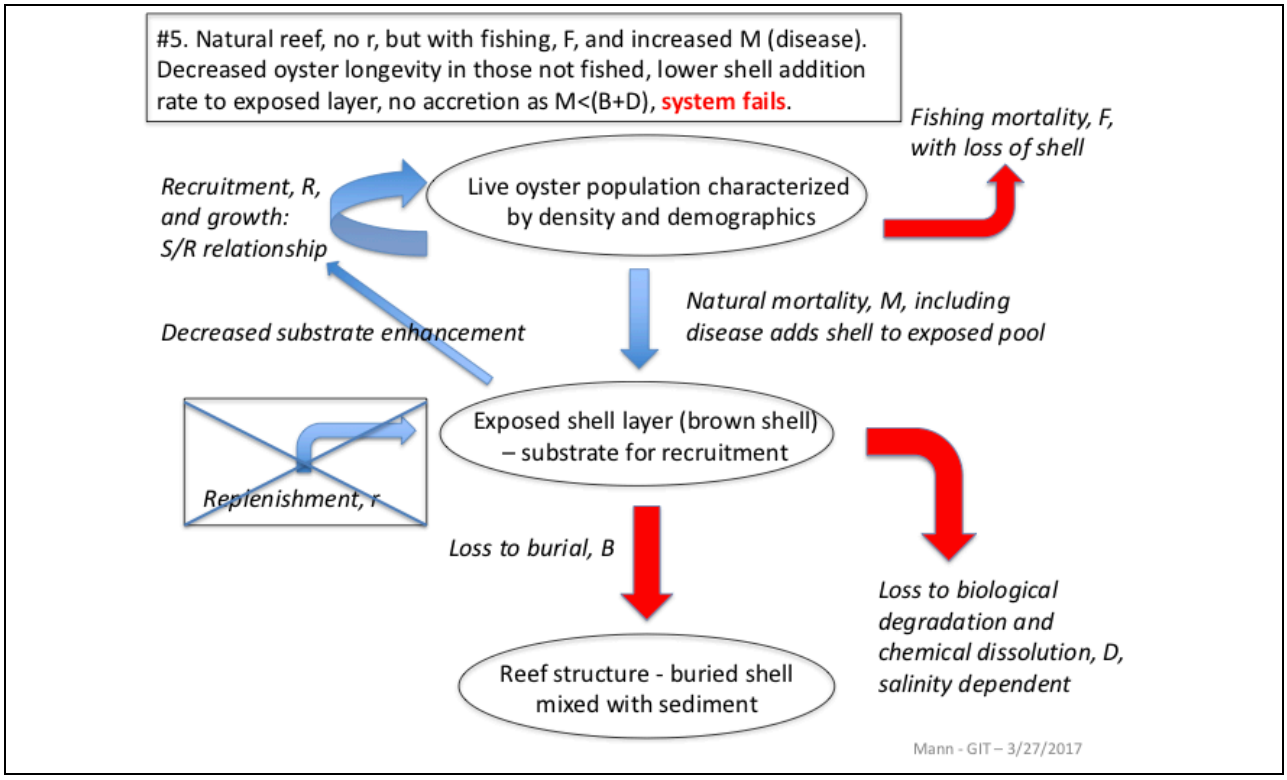
#5. Natural reef, no r, but with fishing, F, and increased M (disease). Decreased oyster longevity in those not fished, lower shell addition rate to exposed layer, no accretion as M<(B+D), system fails.
Fishing mortality, F, with loss of shell
Recruitment, R, and growth: S/R relationship
Live oyster population characterized by density and demographics
Natural mortality, M, including disease adds shell to exposed pool
Decreased substrate enhancement
Exposed shell layer (brown shell) – substrate for recruitment
Replenishment, r
Loss to burial, B
Loss to biological degradation and chemical dissolution, D, salinity dependent
Reef structure - buried shell mixed with sediment
Mann - GIT – 3/27/2017

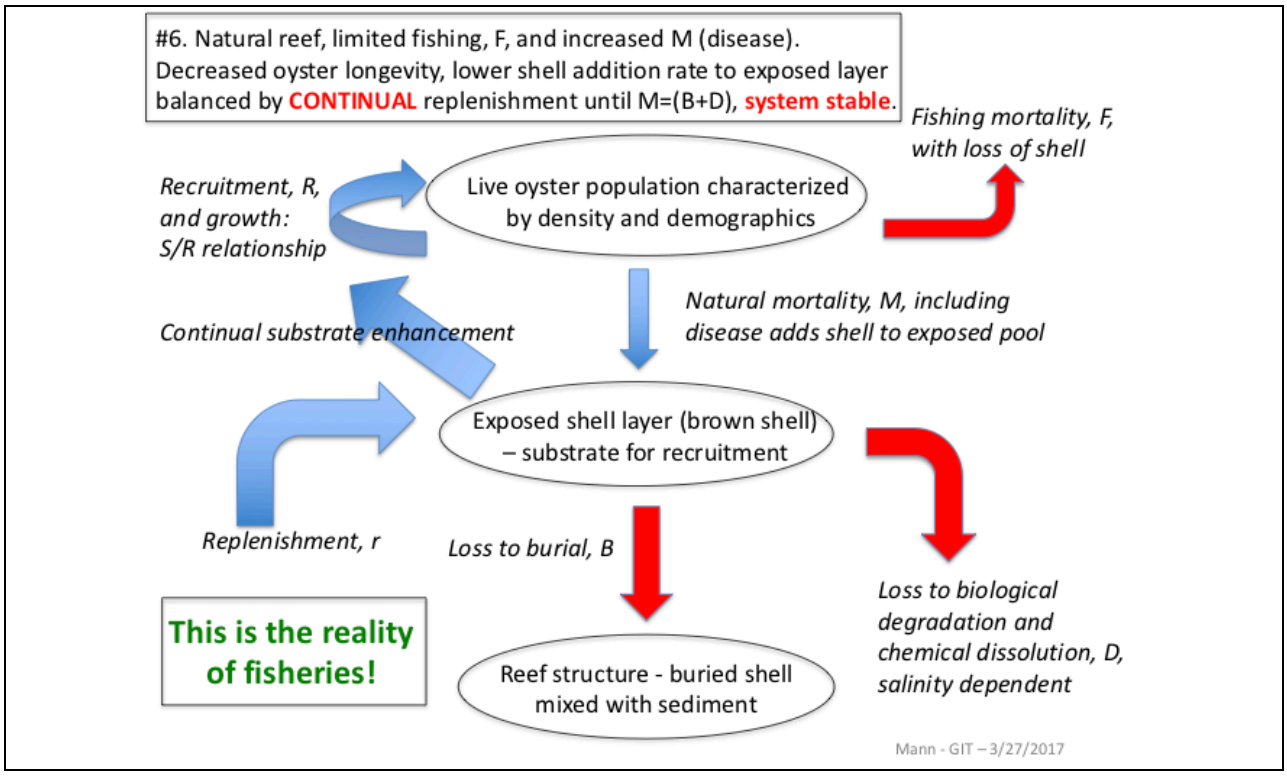

The origins and nature of data for the current study: how they are collected

Maryland data for the current study originate in the Annual Fall Survey Reports. These comprehensive reports are available at https://dnr.maryland.gov/fisheries/Pages/shellfish.../reports.aspx.

Briefly, these are dredge surveys that employ short duration tows on target reefs with examination of both live oyster and shell resources retained in each tow. Tows are timed at fixed steaming rates and thus swept area per tow is estimated. Thus catch can be expressed as oysters or shell per unit area. Individual oysters are classified as spat (Young of The Year, YOY), small (<75mm SL), or market (>75mmSL) categories and sub samples are measured for SL. This study employed data collected in the year 2010-2015 because data were available in 2mm length intervals. Prior to these years data were recorded in 5mm intervals, which compromised the ability to discriminate year classes within the population. The 2010-2015 interval was more than adequate to provide a base for estimation of growth rate and thus discrimination of year classes that are the prerequisite to shell budgeting as described earlier. Note that these surveys collect additional information of "boxes" – articulated valves of dead oysters. There is a traditional approach to estimating mortality using "box counts". While this is a useful relative approach it is debatable as a quantitative measure of mortality rate in that disarticulation rate of valves is size dependent and poorly documented. Given that the half-life of a "box" is not well documented it cannot be used to estimate shell addition to the underlying reef. In the current study shell addition is based on estimated of mortality generated by loss from a cohort with time as described above. The swept area derived estimates of shell density per unit area are arguably underestimates of total shell presence because the dredge collects from the surface of the reef area, it does not and was not designed to penetrate through to the underlying black shell. Thus we can expect proportions of live oysters (as shell) to brown shell (that above the sediment water interface and the result of recent mortality) to show bias towards the live oyster value. This

compromises the ability to estimate loss of brown shell to taphonomy, but all is not lost in that the oyster live shell can be parsed into production and mortality on an annual basis and the dynamic rate of shell turnover estimated from the survey data.

Virginia data originate in the Annual Fall Patent Tong Surveys. The survey protocol is described in Mann et al (2009b) and the data are reported on the Virginia Oyster Stock Assessment and Replenishment Archive (VOSARA) web portal at cmap2.vims.edu/VOSARA/viewer/VOSARA.html.

The patent tong survey employs a stratified random survey design with individual tong deployments in each strata. The tong samples a one square meter area. The number of tong deployments per strata is based on a minimum sampling numbers following the procedure of Bros and Cowell (1987). Retained material is described as live oysters (YOY=spat, small, and market oysters, all measured to nearest mm SL), "boxes" (again to nearest mm SL), brown shell (that above the sediment water interface in the oxic zone, volume in L), and black shell (that below the sediment water interface in the anoxic zone, volume in L). The fact that the tong penetrates to the base of the brown shell layer (as evidenced by the collection of underlying black shell) allows the dynamic of shell in both the live oyster and brown shell components to be examined on a unit area basis. The black shell measure is arguably underestimated in that it presumably extends deep into the reef base and below the penetration depth of the tong. Data for the current study is years 2006-2016. These years have data collected in mm SL intervals and are post the major epizootic of 2003-2005.

Assembling the data and examining analysis options.

The VA (VIMS) historical oyster assessment master database was assembled by Melissa Southworth and John Thomas from several separate component databases. Southworth refined the shape files corresponding to the sampled reef systems in the VIMS master database to provide corresponding area information. A complete copy of the MD DNR historical database was provided by Mitch Tarnowski to VIMS (Southworth and Thomas) and was reformatted to correspond to the VIMS master simply to facilitate analysis by scripts written by Mann and Thomas. Again, note that the MD data was never collected with the current analysis in mind – it is based in a data stream that has served MD management well for many years. Not all stations had data sets with individual oyster shell lengths included and a few employed pooled samples for shell length from more than one dredge tow. These were excluded from the analysis. Final analysis was based on 925 stations (141, 162, 156, 146, 140 and 180 in years 2010 through 2015 respectively).

Having assembled the master databases, the next step in developing a shell budget was to assess options for aggregating or not data from the many reef systems represented therein. Not only does this reduce computational time but it provides categories of data by area or river system.

The above described databases are rich resources for analysis in that they include comprehensive length demographics as described, plus additional subsampling for a suite of individual descriptors including whole animal shell length (as mentioned), shell width, shell height, wet and dry shell weight, wet and dry meat (tissue) weight, and ash (inorganic fraction) tissue weight. Not all are important for the current purpose. To develop a shell budget the priority data are the shell lengths (the general descriptor for all collections) and the dry shell weight (shell volumes can be generated from weight if the desire is to work in volume rather than weight, although both are equally tractable herein). Corresponding data streams for both length and weight parameters are available for 22 reefs in MD for 2011-2013 (n = 25 for each reef for each year, total n = 75 per reef) and for 62 reefs in VA for 2010 and 18-20 reefs for 2011-2016 (again n = 25 for each reef for each year). The shell length versus dry shell weight relationships were explored using power relationships where y (shell weight) = a*(shell length)^b. The exponent b incorporates both the variation in shape of the oyster. Where b = 2 exponent the shape is a tube whereas b = 3 is a sphere, for a comprehensive review of b exponents in oysters see Powell et al (2015). The constant "a" in the power function generally explores shell thickness, although it is a very small value. The shell thickness is also

incorporated in the exponent b value in that shell thickness also increases with size. Thus a spherical shape with increasing shell thickness can generate b values in excess of 3. A general consideration of both shell thickness and oyster shape is important in the development of an oyster shell budget as the assemblages of graphics Figure 2 illustrates. Start with a sample demographic for one year and consider the presence of five-year classes, the overlap of the year classes, and the mortality. Then progress to two demographics for sequential years. Finally, apply differing allometric relationships based on observations from the Lower and Upper James River (data in tabular form later in the text). Note how both the absolute quantity of shell changes and the distribution of shell mass changes between the year classes.

Can we or should we aggregate these data from single reefs to regional values? For each data set (MD and VA) shell length, weight, dry meat weight, wet shell weight and dry shell weight data were plotted by individual year and reef, then aggregated by year for each reef. In several instances' small reefs in immediate proximity to one another in the VA data set have been pooled (e.g., Mobjack "All" and Tangier "All") so the number in the summary table is less than the number given in the above paragraph. The fitted allometric relationships are described in Tables 4 through 7 below.

The 22 MD reefs present a general continuum of decreasing values of the constant "a", with increasing values of b, the latter gradually increasing from 2.18 (all years included) at Lancaster to 2.95 at Hacketts. Various aggregation options were considered in analysis (for example should we consider Old Field + Ware Rock + Wilson Island (b = 2.395 – 2.42) as a single unit?); however, when growth analysis dictated employment of a single age versus length curve for all reefs the decision was made to examine each reef shell budget as a unique location. Note that b values for shell data do not correspond to the same ascending order as b values of dry meat weight. Shell weight accumulates whereas meat weight varies seasonally with food availability and spawning. Meat weight accumulation may also be more sensitive to sedimentary load, salinity and/or other environmental variables. This is the difference in "condition" alluded to in Table 3 on page 7 of this report.

Aggregation of the VA data based on shell weight and meat weight b values was also examined. In VA, 2010 was an unusually wet year, thus while the ranked order of the reefs should be representative of a multi-year data set the absolute b values may not necessarily be near the means for the 2010-2016 period. Reef a and b values were estimated and subsequently ranked on the b value, then compared among the 2010 alone and 2010-2016 (all year combined) values within river systems. For the Great Wicomico (GWR in tables below) there is general agreement between 2010 and combined values (long term shell weight b values in the middle of a range from 2.73 – 3.275). Long term shell weight b values for the Piankatank (PR in tables) are in the 2.96-3.26 range with one exceptional year (2010) for Palace Bar where b is driven by 3 high points in the plot. Rappahannock River (RR in tables) shell b values generally increase in a downstream cline with most values being in the range 2.88 – 3.28. York River shell b values are between 2.75 and 2.98. Pocomoke and Tangier b values are between 2.79 and 3.12. All limited ranges encourage aggregations into larger data pools by year and reef in the river systems described. The James River (JR in tables) shell b values suggests an aggregation of upriver reefs (Moon Rock, Lower Horse Head (LHH), Upper Horsehead (UHH), Middle Horsehead (MHH), Triangle reef, Point of Shoals (POS), and V Rock – Mulberry is an outlier here having a higher b = 2.76 driven by two unusual x,y points), middle river reefs (Lower Jail Island, Cross Rock, Swash, Dry Lumps, Days Point, Hotel Rock and Shanty) and down river reefs (Snyder's, Wreck Shoals, Thomas Rock, Cruisers, Brown Shoal, Nansemond Ridge).

2010 shell b values for Upper Deep Water Shoals, Upper Jail Island and Offshore Jail Island provide single year high b values driven by 2-3 data points, although Upper Deep Water Shoal (the only one of this trio for which we have multi-year data) sits with lower b value reefs in the multi-year estimator.

Figure 2: An illustration of the influence of shell allometry on shell mass and contributions of year class structure to overall shell budgets.

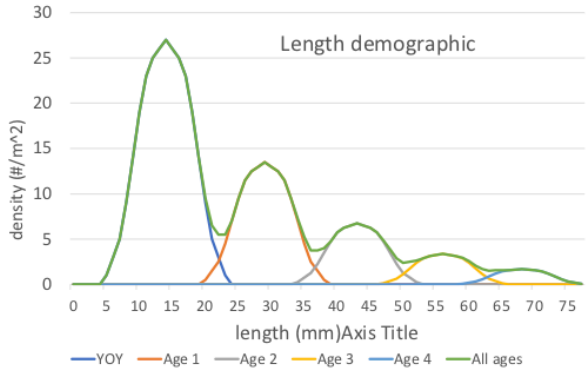

By the numbers:

- The overall demographic (green line) provides total #/m^2
- The demographic is the cumulative of five year classes (YOY through age 4)
- Note overlap of year class sizes.
- The decreasing # in each year class provides estimate of mortality rate (here set at 0.5/y).

Consider these two identical demographics as two sequential years (***to*** and ***t1***): a year class **decreases** in #/m^2 (mortality, **M**), but the live oyster weight of shell increases (in later slide). Shell lost to M is added to the shell base. The challenge is to estimate the magnitude of the addition - is it the # of animals lost to M * weight per shell at YOY or weight of shell at age 1 (when does the oyster die?). This calculation is for the sum of all present year classes at each year transition.

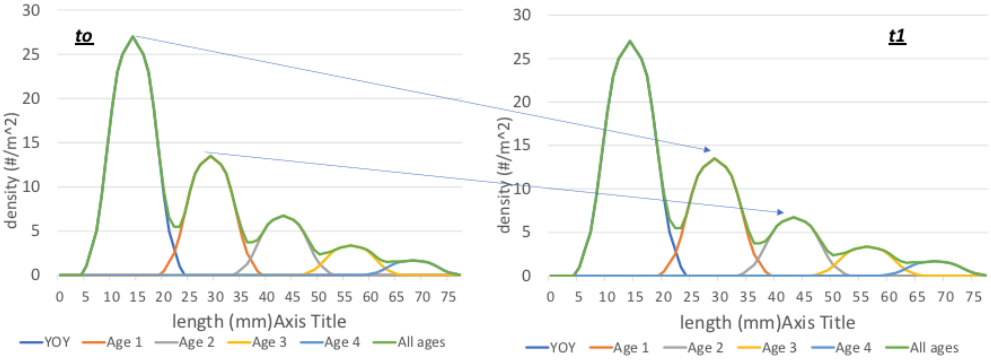

From the length demographic we can estimate shell contribution by length interval and/or year to the total providing we know the length versus shell weight relationship. But what is the shape of that relationship? It varies approximately between that of a cylinder and that of a sphere, or b exponent values between 2 and 3 when expressed as the allometric equation W = a*L^b where W = weight, L = shell length, and both a and b are constants.

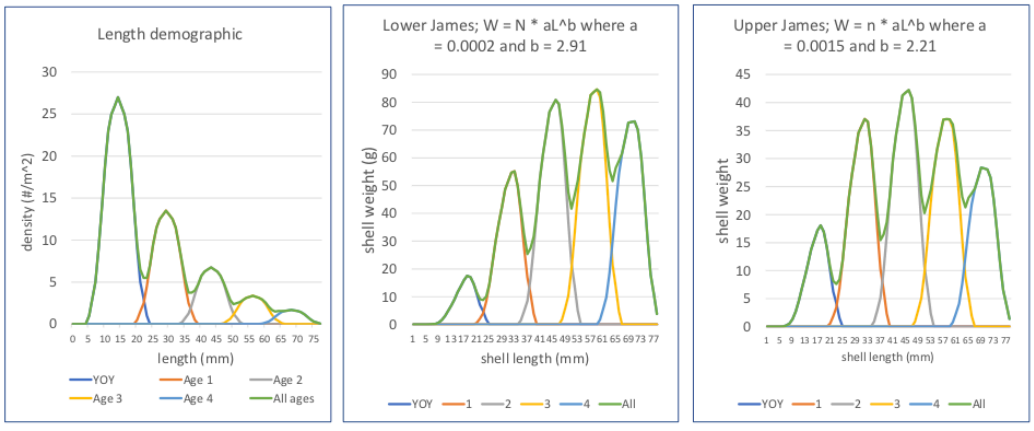

Table 4: Reef specific allometric descriptors for the relationships between shell length (SL, mm) and dry shell weight (DSW, g), and shell length (SL, mm) and dry meat weight (DMW, g) for MD Chesapeake Bay reef systems 2011-2013. See text for additional details.

Maryland Chesapeake Bay reef systems: 2011-2013

All data: ranked by river and b value: shell length v shell weight

Reef	a	b	r^2
Lancaster	6.7E-03	2.18	0.65
Old Field	2.3E-03	2.39	0.80
Ware Rock	2.0E-03	2.41	0.81
Wilson Island	2.0E-03	2.42	0.85
Punch Island	1.4E-03	2.52	0.79
Cason	1.2E-03	2.52	0.85
Pagan	1.1E-03	2.53	0.86
Deep Neck	1.2E-03	2.55	0.81
Lower Cedar Point	1.2E-03	2.57	0.92
Oyster Shell Point	1.2E-03	2.58	0.89
Double Mills	1.1E-03	2.58	0.89
Point Lookout Sanctuary	9.0E-04	2.58	0.81
Tilghman Wharf	6.0E-04	2.71	0.86
Sandy Hill	5.0E-04	2.73	0.94
Piney Island	5.0E-04	2.73	0.88
Sharkfin Shoal	5.0E-04	2.75	0.84
Goose Creek	5.0E-04	2.75	0.85
Broomes Island	5.0E-04	2.76	0.91
Stone Rock	4.0E-04	2.82	0.88
Normans	3.0E-04	2.91	0.85
Turtleback	2.0E-04	2.93	0.94
Hacketts	2.0E-04	2.95	0.91

All data: ranked by river and b value: shell length v dry meat weight

Reef	a	b	r^2
Lower Cedar Point	1.8E-03	1.54	0.60
Old Field	2.0E-03	1.55	0.42
Sharkfin Shoal	4.0E-04	1.85	0.63
Point Lookout Sanctuary	5.0E-04	1.85	0.55
Pagan	2.0E-04	2.00	0.50
Ware Rock	2.0E-04	2.05	0.63
Deep Neck	1.0E-04	2.19	0.59
Turtleback	1.0E-04	2.20	0.82
Hacketts	9.0E-05	2.23	0.63
Normans	9.0E-05	2.24	0.64
Double Mills	9.0E-05	2.26	0.58
Oyster Shell Point	1.0E-04	2.29	0.76
Punch Island	6.0E-05	2.35	0.44
Sandy Hill	5.0E-05	2.35	0.82
Cason	4.0E-05	2.41	0.55
Piney Island	3.0E-05	2.41	0.58
Stone Rock	5.0E-05	2.43	0.81
Wilson Island	2.0E-05	2.52	0.70
Broomes Island	2.0E-05	2.54	0.66
Goose Creek	2.0E-05	2.59	0.65
Tilghman Wharf	1.0E-05	2.76	0.86
Lancaster	5.0E-06	2.88	0.53

Table 5: Reef specific allometric descriptors for the relationships between shell length (SL, mm) and dry shell weight (DSW, g), and shell length (SL, mm) and dry meat weight (DMW, g) for VA Chesapeake Bay reef systems in Pocomoke, Tangier and Rappahannock River (RR) for 2010 and 2010-2016 (highlighted). See text for additional details.

Virginia Chesapeake Bay: Pocomoke, Tangier and Rappahannock River

	All data: ranked by river and b value: shell length v shell weight **2010 data is NOT highlighted**				**All data: ranked by river and b value: shell length v dry meat weight** **2010-2016 all data is highlighted**			
River	reef	a	b	r^2	reef	a	b	r^2
Pocomoke	13H2	4.0E-04	2.79	0.84	13H2	3.0E-05	2.43	0.75
	All	9.0E-05	3.12	0.96	All	3.0E-05	2.49	0.83
Tangier	California	2.0E-04	2.95	0.93	All	6.0E-05	2.28	0.76
	All	1.0E-04	3.04	0.95	California	6.0E-05	2.30	0.76
RR	Ross	3.6E-03	2.24	0.94	Ross	6.0E-04	1.88	0.78
	Broad Creek	6.0E-04	2.65	0.89	Broad Creek	2.0E-04	1.97	0.70
	Bowlers	8.0E-04	2.67	0.88	Ross	1.0E-04	2.24	0.82
	Ross	8.0E-04	2.67	0.93	Bowlers	1.0E-04	2.27	0.74
	Long Rock	3.0E-04	2.86	0.90	Broad Creek	5.0E-05	2.34	0.83
	Broad Creek	2.0E-04	2.87	0.91	Temple Bay	3.0E-05	2.42	0.78
	Temple Bay	2.0E-04	2.90	0.92	Parrot	3.0E-05	2.45	0.83
	Parrot	2.0E-04	2.93	0.89	Long Rock	3.0E-05	2.50	0.92
	Drumming	2.0E-04	2.98	0.87	Morattico	2.0E-05	2.56	0.82
	Drumming	1.0E-04	3.04	0.85	Drumming	1.0E-05	2.66	0.90
	Morattico	1.0E-04	3.08	0.94	Drumming	9.0E-06	2.76	0.86
	Parrot	4.0E-05	3.28	0.90	Parrot	6.0E-06	2.88	0.92
	Smokey Pt	1.0E-05	3.56	0.92	Smokey Pt	1.0E-06	3.17	0.88
	Morattico	8.0E-06	3.74	0.94	Morattico	2.0E-06	3.18	0.94

Table 6: Reef specific allometric descriptors for the relationships between shell length (SL, mm) and dry shell weight (DSW, g), and shell length (SL, mm) and dry meat weight (DMW, g) for VA Chesapeake Bay reef systems in James River (JR) for 2010 and 2010-2016 (highlighted). See text for additional details.

Virginia Chesapeake Bay: James River

All data: ranked by river and b value: shell length v shell weight
2010 data is NOT highlighted

River	reef	a	b	r^2
JR	Moon	7.3E-03	1.85	0.84
	MHH	6.0E-03	1.87	0.91
	Triangle	3.3E-03	2.00	0.89
	POS	3.4E-03	2.02	0.68
	UHH	3.3E-03	2.02	0.85
	MHH	1.8E-03	2.15	0.88
	POS	1.8E-03	2.16	0.84
	LHH	1.6E-03	2.23	0.85
	V Rock	1.2E-03	2.27	0.86
	Wreck	2.0E-03	2.29	0.69
	Lower Jail	1.8E-03	2.36	0.92
	Upper DWS	8.0E-04	2.37	0.76
	Cross	1.0E-03	2.42	0.88
	Swash	1.0E-03	2.44	0.86
	Dry Lumps	8.0E-04	2.53	0.87
	Days	5.0E-04	2.67	0.93
	Swash Mud	2.0E-04	2.72	0.90
	Off Swash	5.0E-04	2.72	0.91
	Mulberry	2.0E-04	2.76	0.94
	Hotel	3.0E-04	2.76	0.77
	Shanty	3.0E-04	2.82	0.95
	Wreck	2.0E-04	2.92	0.89
	Cruiser	2.0E-04	2.92	0.95
	Thomas	2.0E-04	2.93	0.93
	Upper DWS	7.0E-05	2.98	0.68
	Nansemond	1.0E-04	3.00	0.92
	Upper jail	1.0E-04	3.05	0.92
	Thomas	5.0E-05	3.22	0.96
	Off Jail	3.0E-05	3.27	0.92
	Brown	3.0E-05	3.31	0.96
	Snyder's	3.0E-05	3.39	0.96

All data: ranked by river and b value: shell length v dry meat weight
2010-2016 all data is highlighted

reef	a	b	r^2
Off Swash	2.0E-04	1.74	0.78
Moon	2.0E-04	1.77	0.74
Wreck	3.0E-04	1.90	0.80
Cruiser	2.0E-05	1.92	0.80
POS	1.0E-04	1.94	0.68
UHH	5.0E-05	2.08	0.81
Swash Mud	5.0E-05	2.09	0.86
Nansemond	9.0E-05	2.10	0.80
Off Jail	6.0E-05	2.14	0.79
Days	1.0E-04	2.15	0.83
MHH	3.0E-05	2.17	0.82
V Rock	4.0E-05	2.18	0.82
Nansemond	7.0E-05	2.20	0.81
Swash	5.0E-05	2.21	0.90
MHH	3.0E-05	2.21	0.85
POS	3.0E-05	2.25	0.84
Cross	4.0E-05	2.27	0.84
Wreck	4.0E-05	2.31	0.79
Upper DWS	2.0E-05	2.35	0.79
Triangle	1.0E-05	2.39	0.87
Thomas	3.0E-05	2.43	0.86
Mulberry	1.0E-05	2.44	0.85
Hotel	2.0E-05	2.48	0.57
Dry Lumps	1.0E-05	2.57	0.77
Brown	1.0E-05	2.59	0.91
Shanty	9.0E-06	2.63	0.84
LHH	5.0E-06	2.65	0.83
Snyder's	1.0E-05	2.70	0.93
Thomas	8.0E-06	2.74	0.94
Upper DWS	4.0E-06	2.79	0.74
Upper jail	5.0E-06	2.81	0.91
Lower Jail	4.0E-06	2.81	0.93

Table 7: Reef specific allometric descriptors for the relationships between shell length (SL, mm) and dry shell weight (DSW, g), and shell length (SL, mm) and dry meat weight (DMW, g) for MD Chesapeake Bay reef systems in Great Wicomico (GWR), Piankatank (PR) and York Rivers (YR), and Mobjack Bay for 2010 and 2010-2016 (highlighted). See text for additional details.

Virginia Chesapeake Bay: Great Wicomico (GWR), Piankatank (PR) and York Rivers (YR), and Mobjack Bay reef systems

	All data: ranked by river and b value: shell length v shell weight				**All data: ranked by river and b value: shell length v dry meat weight**			
	2010 data is NOT highlighted				**2010-2016 all data is highlighted**			
River	reef	a	b	r^2	reef	a	b	r^2
GWR	Shell Bar	1.0E-03	2.46	0.76	Cranes	1.0E-04	2.08	0.73
	Sandy Pt	4.0E-04	2.73	0.94	Cranes	8.0E-05	2.15	0.65
	Shell Bar	2.0E-04	2.83	0.87	Shell Bar	6.0E-05	2.16	0.74
	Cranes	3.0E-04	2.83	0.85	Shell Bar	4.0E-05	2.25	0.85
	Fleet	1.0E-04	3.09	0.94	Haynie	5.0E-05	2.27	0.78
	Haynie	8.0E-05	3.11	0.95	Sandy Pt	3.0E-05	2.35	0.86
	Cranes	4.0E-05	3.28	0.91	Fleet	4.0E-05	2.39	0.87
PR	Ginny	2.0E-04	2.97	0.94	Deep Rock	6.0E-05	2.27	0.80
	Deep Rock	1.0E-04	3.03	0.84	Ginny	3.0E-05	2.41	0.88
	Palace Bar	1.0E-04	3.05	0.91	Palace Bar	2.0E-05	2.45	0.85
	Cape Toon	1.0E-04	3.06	0.95	Cape Toon	1.0E-05	2.53	0.88
	Burton Point	6.0E-05	3.19	0.96	Burton Point	9.0E-06	2.68	0.93
	Bland Point	3.0E-05	3.27	0.94	Bland Point	8.0E-06	2.72	0.91
	Heron Rock	3.0E-05	3.27	0.94	Heron Rock	6.0E-06	2.76	0.90
	Palace Bar	1.0E-05	3.56	0.98	Palace Bar	2.0E-06	3.01	0.98
York	Bell Rock	5.0E-04	2.75	0.90	Bell Rock	7.0E-05	2.27	0.83
	Aberdeen	4.0E-04	2.78	0.85	Aberdeen	5.0E-05	2.29	0.28
	Aberdeen	3.0E-04	2.85	0.89	Bell Rock	3.0E-05	2.41	0.91
	Bell Rock	1.0E-04	2.98	0.91	Aberdeen	2.0E-05	2.49	0.80
	Propatank	5.0E-05	3.25	0.98	Propatank	2.0E-05	2.55	0.84
Mobjack	Tow Stake	5.0E-04	2.73	0.92	Tow Stake	1.0E-04	2.32	0.79
Mobjack	All	2.0E-05	3.49	0.93	All	6.0E-06	2.82	0.83

A final note is appropriate on the use of b values as drivers of data aggregation. The r^2 values for individual year-reef plots regularly exceed 0.80, often 0.90, providing confidence in the utility of the approach. The large n values (75-150) provided by multi-year observations also provide high r^2 values indicating general consistency between years. Any such plots are limited by the data ranges, and those examined herein have included shell lengths from 30 mm upwards. Oysters with shell lengths in excess of 100 mm are not abundant in this dataset, thus wide disparities in predicted weights from shell lengths are limited by the length range included. Lengths beyond 100 tend to illustrate the dispersion in estimated shell weight driven

by the change in b value. This is a substantial compilation of plots. A complete depiction of all rivers and years is available if requested by CBT. The final aggregation of sampling areas within the Virginia portion of the bay is illustrated in Figure 3.

Figure 3. Aggregation of sampling area in the Virginia Chesapeake Bay. See text for additional details.

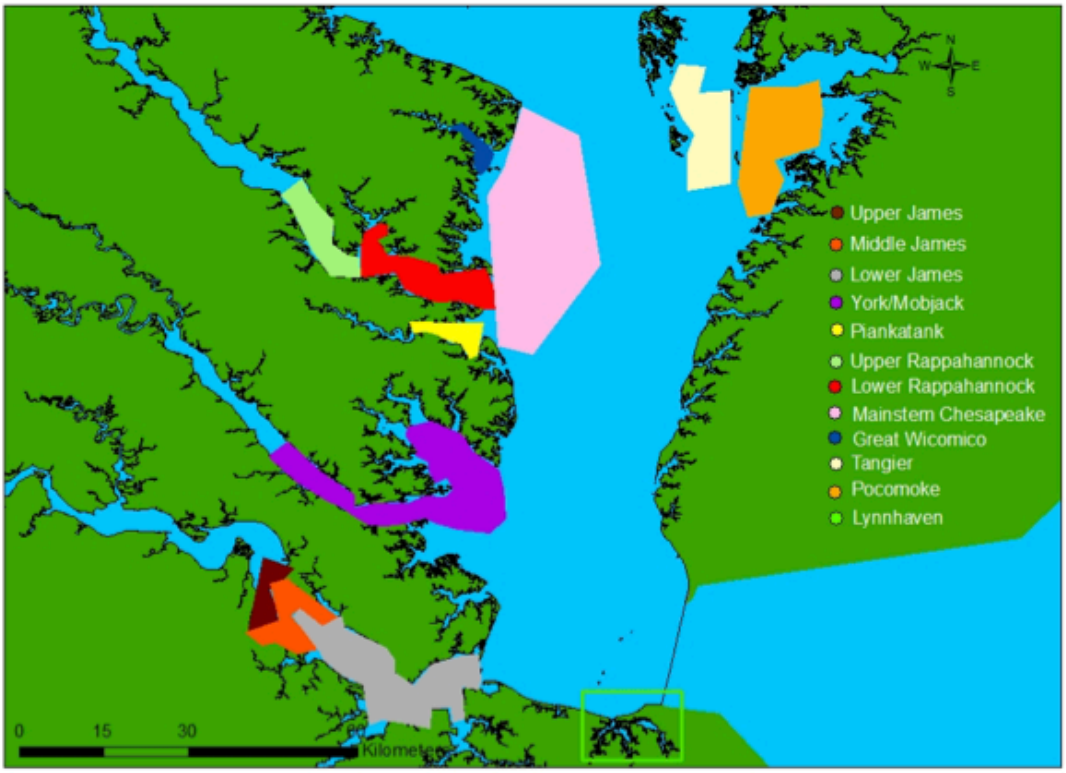

From a demographic plot to length at age and year class structure.

The critical analytical step in the entire shell budget as presented is the ability to generate a year class structure from the demographic plot. Once this step is complete the allometric length to weight relationships allow estimation of biomass and shell standing stock, production and loss rates. Everything else flows from this pivotal section of the analysis.

Bhattacharya (1967) provides a simple method for "resolution of a distribution into Gaussian components" – that is year classes in the distributions presented in these databases. This analytical approach was employed to examine the Virginia data by the area aggregations described above and found to produce reasoned year classes (more on this below). The Maryland data was also examined on an individual reef basis, but the variability in year class strength within the time frame 2010-2015 produced results in that years with few oysters are both good and bad – good in that they allow emphasis of adjacent strong year classes in demographic plots, but bad in that they also over-emphasize the signal from low numbers of individuals that may not be representative of a year class. Eventually all MD data was aggregated on a single plot in Figure 4. This is, again, not perfect. The continuous lines between the year plots join the peaks of identified year classes. Troubling is the actual values of numbers within the progress of a single year class within the 2010 through 2015 time frame. The expected decrease associated with mortality is not

always present suggesting a disparity in sampling efficiency of the dredge across size classes. Recall that this is an aggregated demographic, so there is not equal representation of all reefs with respect to n values of included oysters; however, the large number of oysters included should represent the size distribution reasonably well, so generation of a growth curve is tractable.

Figure 4. MD data, all reefs, 2010-2015 shell length frequency by 2mm intervals with a 6mm smoothing.

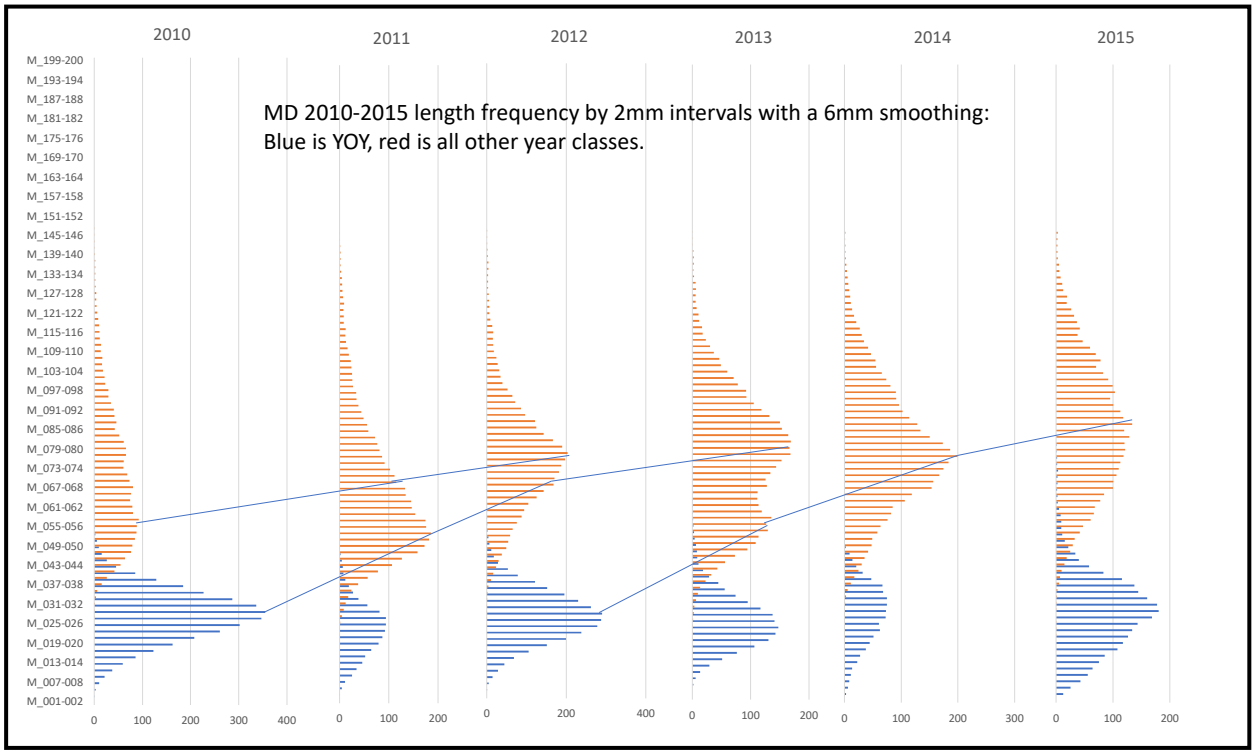

Demographic data was also examined using TropFish R, an R script based on the Bhattacharya (1967) approach. For this analysis the demographic data was presented as 2mm intervals from 2 through 200 mm SL in .csv format for the aggregated MD reefs and the VA aggregated reefs as per the previous description. TropFish R allows the identification of year classes in a simple, sequential high through low point discrimination on the output plots. An example for the MD data is illustrated as a compilation of eight graphics in Figure 5. The sequence of plots identifies peaks in the demographic that correspond to year classes. These peaks are at SL values of 28mm, 58mm, 82mm, 106mm, 122mm, 138mm, 152 mm and 158 mm. Given that surveys are completed in November these peaks correspond to **year classes** YOY and ages 1 through 7 respectively. Assuming a recruitment in the mid-summer June-July period **actual age** is approximately 0.5 y for YOY with +1y increment for each year class (1.5y. 2.5y and so forth). This provides a length (SL, mm) at **actual age** (x, y) plot that is described by the polynomial:

$$SL\ (mm) = -1.714x^2 + 32.33x + 12.59,\ R^2 = 0.999$$

Note the general concordance of the TropFish peaks with the earlier frequency interval plot. The value of the TropFish generated plot is the discrimination of year classes in lengths >100mm SL that are not immediately evident in the frequency plot above. The numbers in each year class were separated by the mid-point between the identified peaks at 43mm, 70mm, 94mm, 114mm, 130mm, 145mm, and 155mm. Thus all <43 mm SL = year class 1, 44 mm through 70mm SL = year class 2 and so forth.

Figure 5. An illustration of year class identification in MD data using TropFish R. See text for additional details.

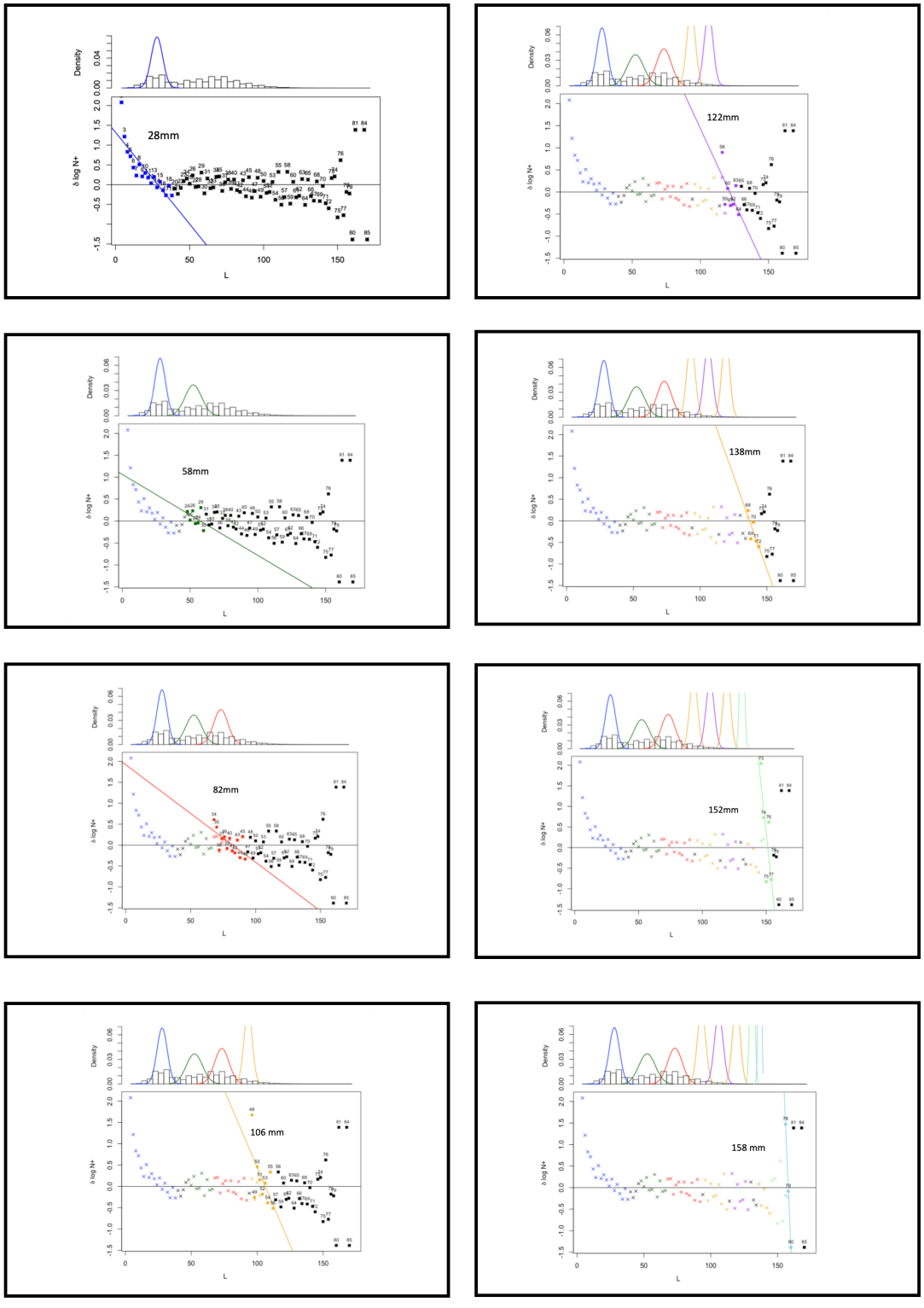

The above procedure was repeated for each of the identified region (aggregations) in the VA data sets. The following length (SL, mm) at **actual age** (x, y) descriptors were generated. Effectively all have $R^2 = 1$. Note these are NOT von Bertalanffy (1938) fits with K and L_{inf} values – given the general disregard for consistent allometry by oysters this is not at all surprising (again, see Powell et al 2015).

Tangier	SL (mm) = $-2.84x^2 + 36.36x + 0.22$
Pocomoke	SL (mm) = $-2.3x^2 + 36.42x + 2.14$
Rappahannock regions 1-5	SL (mm) = $-2.43x^2 + 33.36x + 6.42$
Rappahannock region 6	SL (mm) = $-2.84x^2 + 36.36x + 0.22$
Great Wicomico River	SL (mm) = $-1.15x^2 + 25.2x + 7.87$
Piankatank River	SL (mm) = $-1.93x^2 + 28.28x + 4.88$
York River & Mobjack Bay	SL (mm) = $-1.68x^2 + 30.48x + 1.04$
Lower James River	SL (mm) = $-1.37x^2 + 26.93x + 1.74$
Middle James river	SL (mm) = $-1.5x^2 + 30.3x - 0.98$
Upper James River	SL (mm) = $-1.7x^2 + 28.6x - 0.64$

A worked example: Piankatank River 2006-2016.

Below I describe a worked example for the Piankatank River for the 2006-2016 period. Figure 6 is a time series demographic plot, the horizontal axes for each year are not constant reflecting changes in year class strength. Blue is YOY, all other year classes in orange. Follow the peaks of year classes as they progress through time. There are 67,551 oysters from 807 stations represented in these plots. Note the progression of the year classes through the time series. The peak heights can be identified by the graphical procedure of Bhattacharya (1967) or the TropFish R option. Once the growth curve is overlain on the demographic data the year classes can be identified and a mortality curve for each year class estimated.

Figure 6. Time series demographic of oyster in the Piankatank River. Blue is YOY, all other year classes in red. See text for additional details.

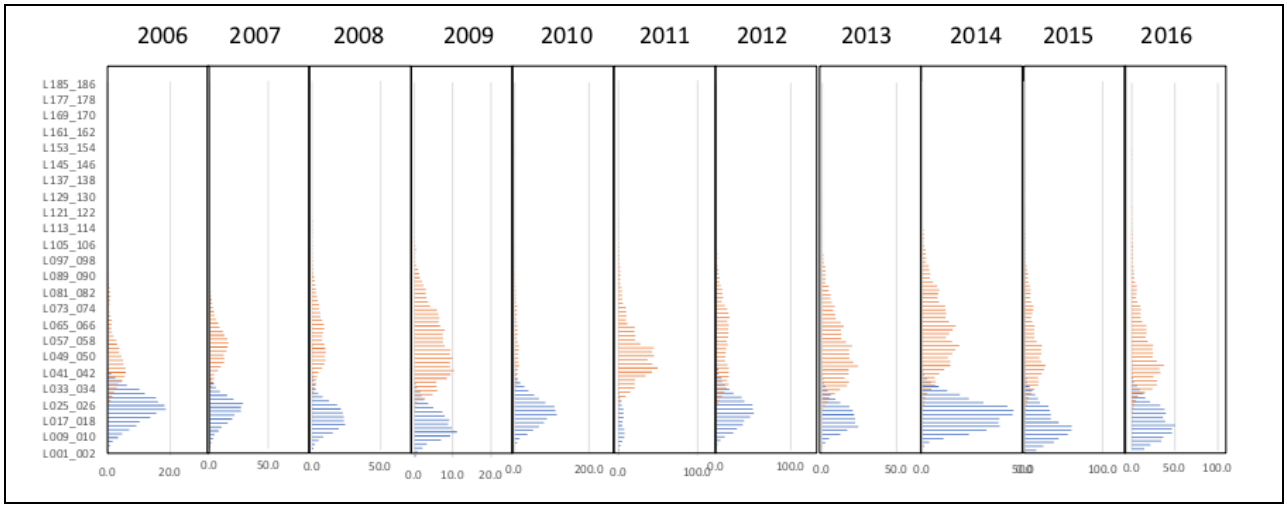

Figure 7 (below) is a compilation of four graphics that illustrate respectively the age at length, percentage survival (1-mortality), and shell length versus dry meat (SL v DMW) and shell length versus dry shell weights (SL v DSW) for the 2006-2016 period for the Piankatank River oyster. This is for a age truncated population. Note the approximation to a declining exponential of the survival curve of the survival

curve.– the important of this curve will be revisited later in the text with respect to evolutionary ambit of oysters.

Figure 7. Piankatank River oysters, 2006-2016. Age at length, percentage survival (1-mortality), and shell length versus dry meat (SL v DMW) and shell length versus dry shell weights (SL v DSW).

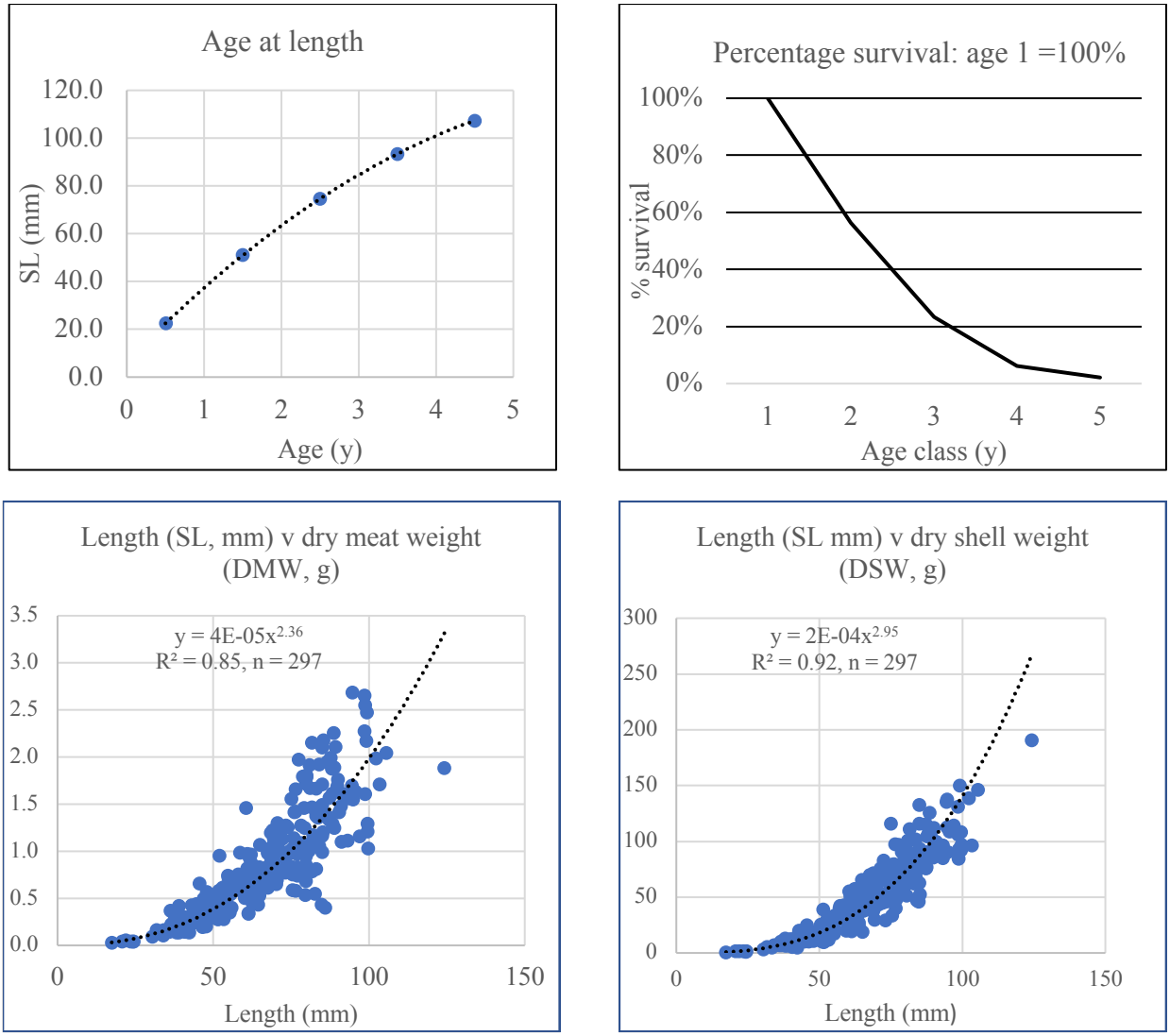

Once the demographic is parsed into year classes then the shell mass and volume associated with live shell by length and year class can be estimated using the allometric relationships. The distribution of shell mass by length for the entirety of the 2006-2016 period is illustrated in Figure 8 below. Note how the values higher than ~80 mm shell length decreases despite the increase in weight per shell. The mortality of animals in this size range (>3y old) underscores the importance of even marginal increases in survival to 4 or even 5 years old to the shell resource. Later in this report each reef (MD) or reef aggregation (VA) is presented individually, and the importance of this age/size truncation discussed.

Figure 8: Piankatank River oysters: shell weight demographic for 2006-2016. See text for additional details.

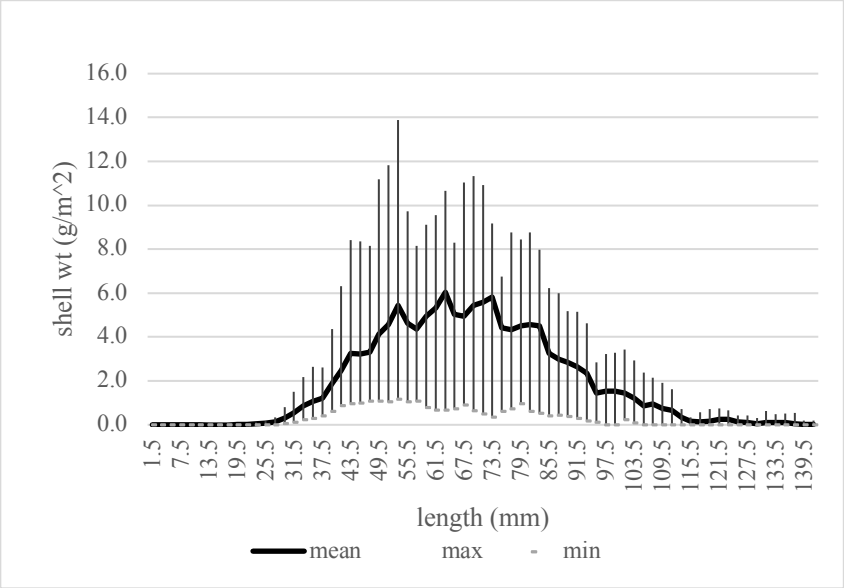

The partitioning of shell volume (in bushels) is illustrated in Figure 9A by sequential years in parallel with volumes of brown (oxic) and black (anoxic) shell layers, plus a total value. This is expressed as **total for the river system** based on shell m^{-2} and total habitat area – note that this plot is only available for VA locations in that the MD data does not include estimates of reef area. This can be addressed on a unit area basis for MD data and I will return to this subject later in the text. What is notable about the VA long-term plot is the **apparently** (this word choice is intentional) stable relationship between the three components with the exception of a modest increase in brown shell in the 2010-2012 period, with subsequent small increases in the live component before all components move back to approximately 2006-2010 values in 2014-2016. When considered on a unit area basis these are low, generally <10L on shell m^{-2}, about one shell thick if considered as a uniform layer.

Figure 9A. Piankatank River: partitioning of shell volume (in bushels) 2006-2016 as live shell, brown (oxic) and black (anoxic) shell layers, plus a total value.

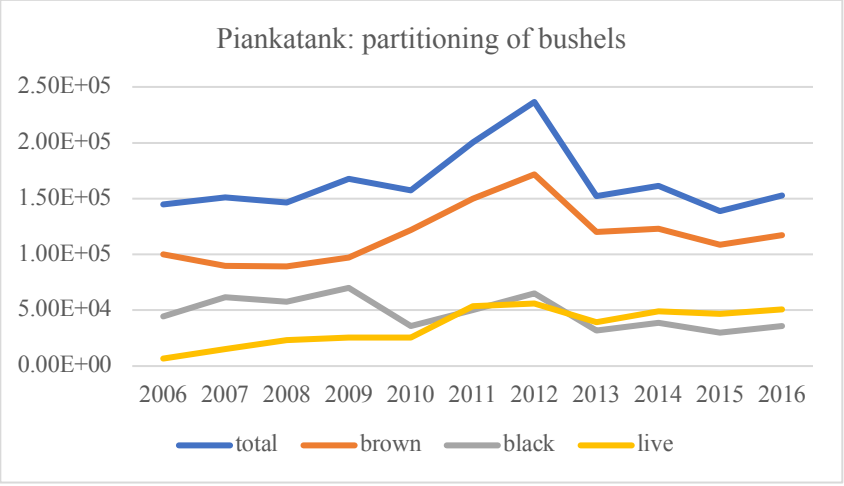

This pattern is indeed replicated in most of the nine VA regions (Figure 9B) for which such plots can be constructed (see below). Lynnhaven and the mainstem data sets are too short or fragmented to provide long term plots.

Figure 9B. Virginia Chesapeake Bay: partitioning of shell volume (in bushels) 2006-2016 as live shell, brown (oxic) and black (anoxic) shell layers, plus a total value.

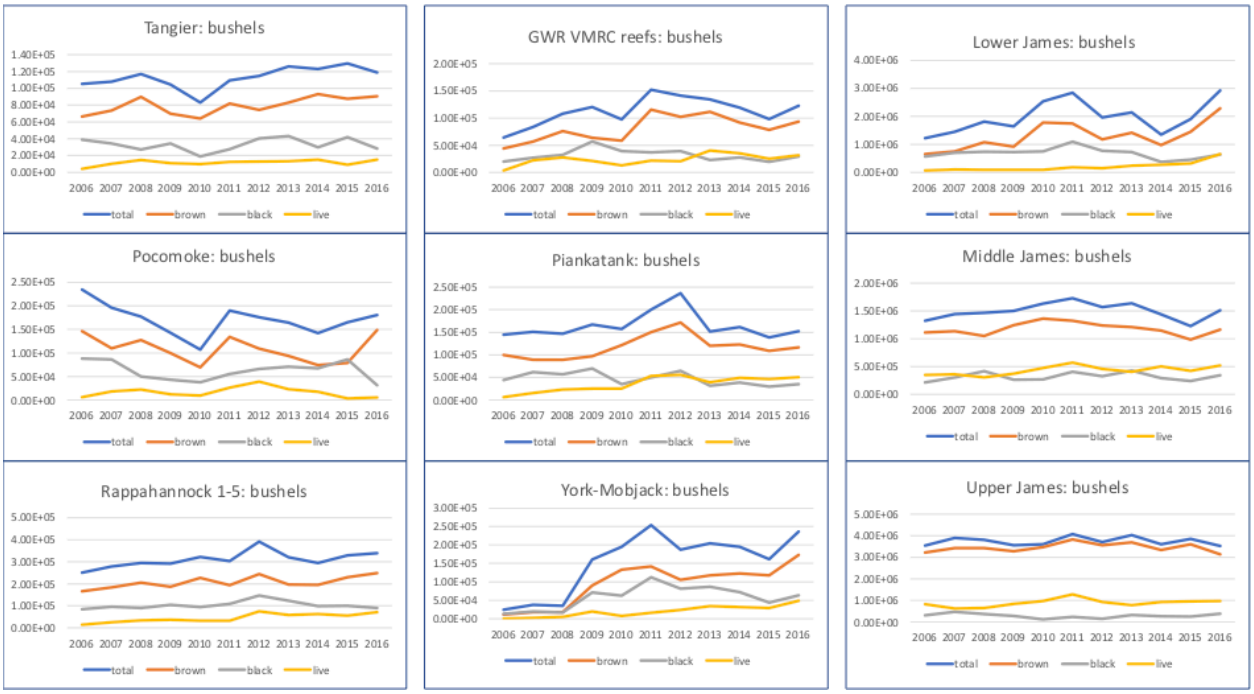

The notable exception is the York-Mobjack region where the plots illustrate the large shell planting and repletion efforts from 2008 onwards. Those stable areas where repletion is not active, for example the James River, all show remarkable stability over time. A region-specific plot of time series observations of live shell versus brown shell (Figure 10) again illustrates the **equilibrium** *(this is an important term to which I shall return)* of the budget components along a fixed relationship. Diversions from this relationship, driven by repletion or unusual recruitment, return in a hysteresis like manner as subsequent shell loss rates from the brown pool exceed the ability of recruitment, growth and mortality to maintain an expanded shell base. Two subtle points emerge from a close examination of Figure 10 – within the range portrayed the addition rates to the brown shell pool from mortality generally match the loss rates to taphonomy and burial, and the intercept of the plot on the x axis suggest a base brown shell values that corresponds to no live shell component. That is there is a residual brown shell value that agrees with the preservation "boundaries" described Powell et al (2012). Note that Figure 10 describes an equilibrium but it does not give the rates of transfer of components in that equilibrium – this I will address in a subsequent section.

I have thus used the example of the Piankatank to indicate an **equilibrium** stability in the shell resource and indeed extended the argument to all of the VA at the **whole river system level**. I cannot complete such an exercise for MD data at this point because of the lack of reef area data, but we will return to this subject shortly in a subsequent analysis that covers all MD and VA data.

Figure 10. Virginia Chesapeake Bay, 2006-2016: Time series observations of brown shell volume (L m^{-2}) versus live shell volume (L m^{-2}).

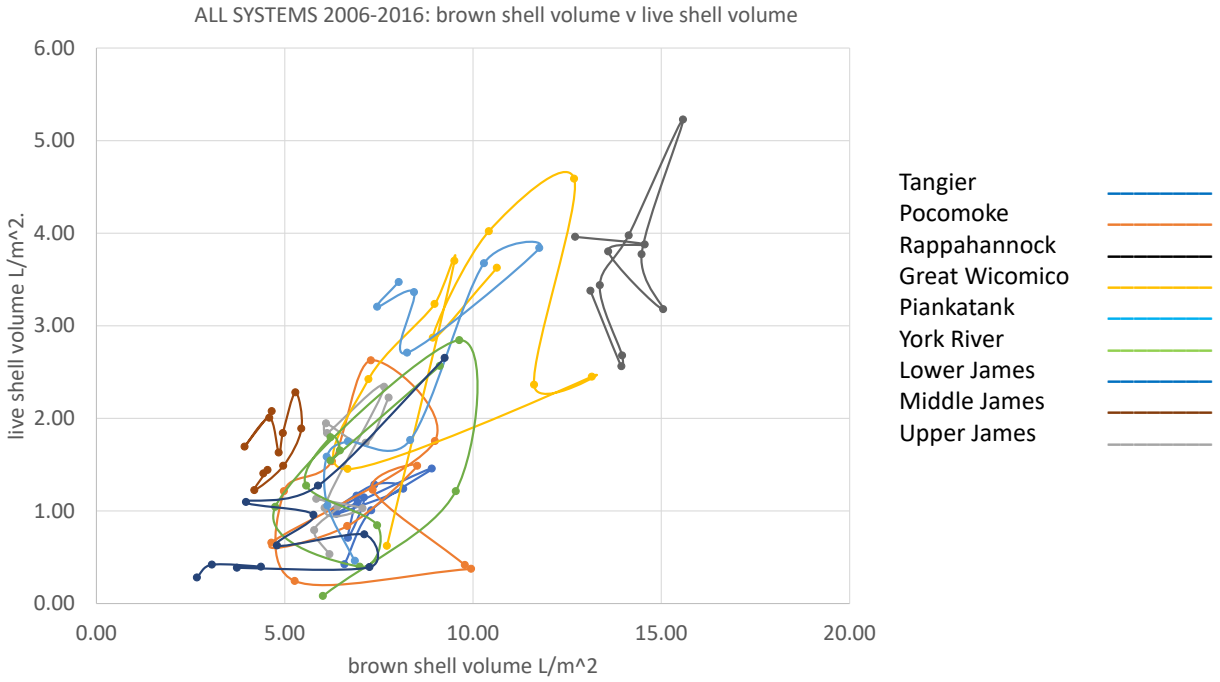

Equilibria and shell dynamics between system components.

The **equilibrium** between the various components of the shell system as described in Figure 1 of this report entitled "A graphical depiction of options" and in the section above entitled "A worked example: Piankatank River 2006-2016" is the result of underlying recruitment, growth and mortality rates. In this section I examine the interplay of these rates in more detail. The demographics from the TropFish output were used to delineate year classes by shell length intervals for all of the MD reefs and the VA aggregations. The length to shell weight allometric relationships were then used to estimate shell weight per unit area for each year class within a sample for each reef/year combination. For MD data this is sampling years 2010-2015, and for VA this is 2006-2016. Given that, for example, the 2010 MD data includes YOY through age 4 oysters, then this sample includes data on year classes 2006 though 2010 (the 4 year-olds were YOY in 2006). Thus a 2010-2015 **year series** can be reconstituted as **year classes** 2006 through 2015. Similarly VA data from sampling in years 2006-2016 can be reconstituted as **year classes** 2002 through 2016. Figures 11 and 12 illustrate the profiles of dry shell in units of gm m^{-2} for the individual reefs. Note that the ordinates on the plots have a variety of scales to accommodate spatial differences. The color sequences on the plots are standard across all plots for one state; for example the 2012 year class for MD is mid green for all sites. VA reefs systems are labeled with complete names (e.g., Great Wicomico River). The MD site and figure labels correspond to areas thus:

MD reefs systems:

BRC	Broad Creek (Deep Neck)
DOS	Dorchester Shore (Punch Island)
EBN	Eastern Bay North (Normans)
FIB	Fishing Bay (Goose Creek)
HAC	Harris Creek (Tilghman Wharf)

LAA	Lower Anne Arundel Shore (Hacketts + Sandy Hill)
LTS	Lower Tangier Sound (Cason)
MPX	Middle Patuxent River (Broome Island)
MTS	Middle Tangier Sound (Piney Island + Turtleback)
NWR	Nanticoke and Wicomico Rivers (Wilson Island)
SMS	St Mary's Shore (Point Lookout Sanctuary)
TAR	Tred Avon River (Double Mills)
TAS	Talbot Shore (Stone Rock)
UCH	Upper Chester River (Old Field)
UCR	Upper Choptank River (Oyster Shell Point)
UPR	Upper Potomac River (Lower Cedar Point)
USM	Upper St Mary's River (Pagan)
UTS	Upper Tangier Sound (Sharkfin Shoal)
WWR	Wicomico River (Lancaster)

What is immediately and consistently evident from these plots is that they peak at 2 or 3 years of age and that very few oysters survive past 5 years of age. Only the low salinity sanctuary in the upper James shows survival into year classes 3 and 4. This is a system in which shell in the live pool turns over quite rapidly – the contribution of a single year class peaks in 2-3 years and is gone by 4-5 years. The implications of such a dynamic turnover are two-fold. First, lack of longevity limits shell contribution per individual. Second, one or more recruitment failures can place the underlying structure in jeopardy. The **equilibrium** is the end product of these dynamic components, and should not be viewed as indicate of long term stability, but one of rapid substrate turnover that is vulnerable to minor perturbation. The range covered by the ordinates in these plots is modest, less than 1,500 g m^{-2} in VA reefs and ranging between 600 and an exceptional 14,000 g m^{-2} in MD reefs. These are peak values typically maintained for one year in the progression of a single year class description.

Of particular interest in this large spatial comparison is the comparatively (again, a relative term) robust status of most of the MD reefs in comparison to the VA reefs. Why is this the case? The answer lies in two differences between the systems; the allometric relationships and the demographics. The allometric relationships of SL v DSW are compared in Figure 13 in three panels that are respectively depicting MD data for 2011-2013 by individual sites as described in Table 4, VA data for 2006-2010 with all sites combined (the highlighted yellow values in Figure 5-7 earlier), and VA data for multiple sites in the James River for 2010 (Table 6). All plots are SL on the x axis in mm, truncated between 30 and 140 mm SL, versus DSW in g on the y axis. These panels have notable differences. The MD data show strong coherence among all 22 sites examined. For example the spread in SL for a DSW of ~200 g is 100-125mm. The VA 2006-2010 combined data shows a slightly greater spread among the plots with, again, the DSW value of ~200 g corresponding to SL values of 105-135 mm with the exception of 3 data sets which never exceed DSW values of 100 g. In stark contrast to third panel for the James River 2010 data has a marked spread of relationships, but with only eight of twenty five plots show DSW values of ~200 g within an SL range of 105-135 mm. Of the remaining plots only two have DSW values >200 g by SL=140 mm, and five plots have DSW values <100 g by SL =140 mm. So the MD oysters are either more rounded per unit length or have thicker shells or both. At the other end of the scale the James River oysters, particularly those from upriver stations at Middle Horsehead, Point of Shoals and Upper Deepwater Shoals, are both unusually elongate and thin shelled. Again, these emphasize the importance of allometry originally illustrated in Figure 2.

Figure 11. Demographic profile of shell weight per unit area on MD reefs by year class for year classes originating in 2006 through 2015. Note that the plot ordinates have a variety of scales to accommodate spatial differences. The color sequences on the plots are standard across all plots; for example the 2012 year class for MD is mid green for all sites. MD reef labels are given in the accompanying text.

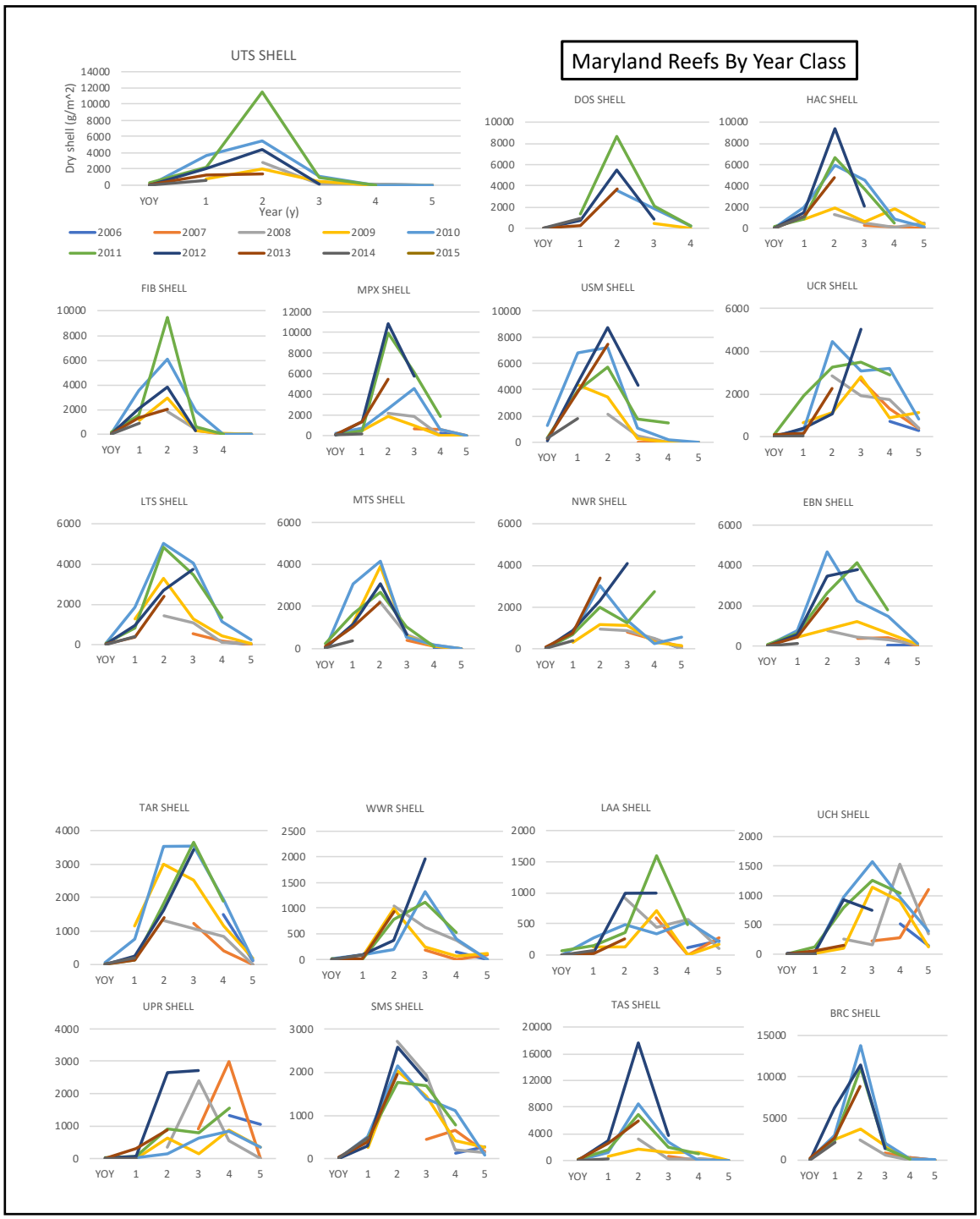

Figure 12. Demographic profile of shell weight per unit area on VA reefs by both year and year class for year classes originating in 2006 through 2016. Note that the plot ordinates have a variety of scales to accommodate spatial differences. The color sequences on the plots are standard across all plots; for example the 2009 year class for VA is orange for all sites.

Figure 13. Allometric relationships of SL (mm) v DSW (g): Left panel -MD data for 2011-2013 by individual sites as described in Table 4. Mid panel - VA data for 2006-2010 with all sites combined (the highlighted yellow values in Tables 5-7), and 2010 VA data for James River (Table 6). All plots are SL truncated between 30 and 140 mm SL on x axis, versus DSW in gm on the y axis.

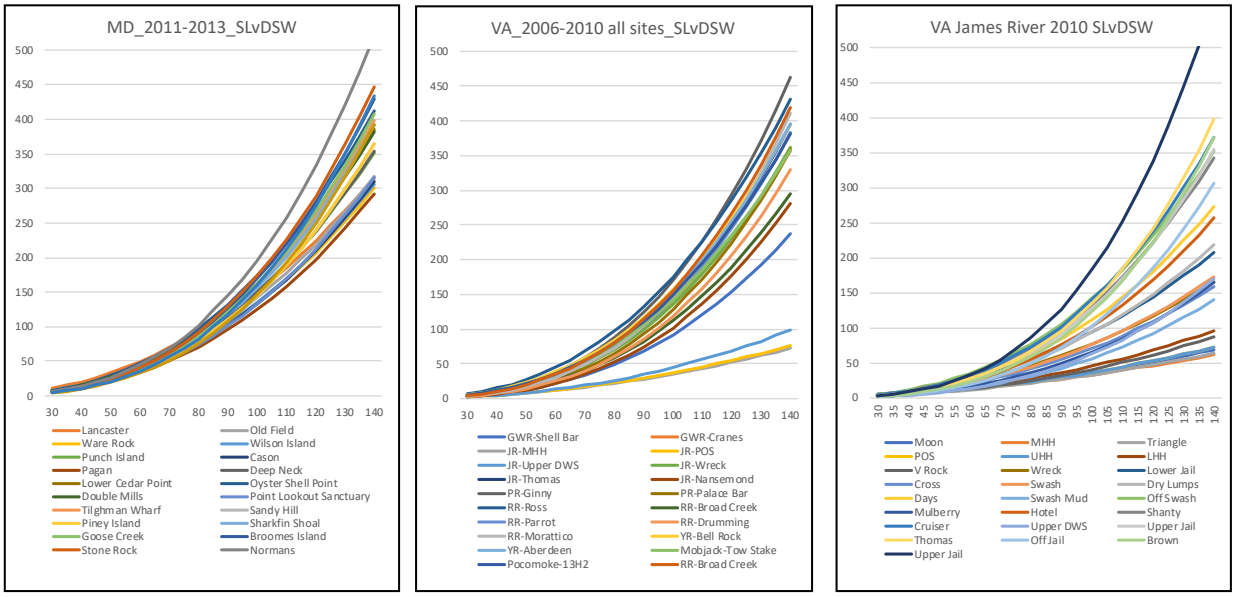

The demographic differences between the state resources emphasize the presence of modest numbers of the largest oysters (>110mm SL) in the MD demographic, including a few >150 mm SL! Such oysters are largely absent in VA collections. When the combination of larger oysters and the allometric relationships described above is considered the disproportionate importance of this modest representation of old and large oysters is obvious.

On the relationship of live shell weight to brown shell weight in extant populations.

At this juncture I return to estimation of the rates of addition and loss to the live and brown shell pools described in Figures 8 through 12. Consider a typical demographic from Figure 11 or 12 with a maximum dry shell density in the range 800-1400 g m^{-2}. Figure 14 provides simulations of that population over a ten year period. Panel A describes survival as a declining function wherein annual mortality, M, is a proportional value between 0.0 (no mortality) and 1.0 (all died). Survival is (1-M) for a period of one year or $(1-M)^q$ for a period of q years. Initial oyster density as YOY is set at 100 m^{-2}, a value typical of the range in the data employed to generate Figures 11 and 12. M values increase in units of 0.02 from 0.58 to 0.72. Survival is <20% by year 2 and mortality essentially complete by year 5. Using the MD composite growth curve generated from Figure 4 and the SL v DSW allometry of oysters from the Piankatank River (Figure 7) a standing stock of shell (dry shell weight m^{-2}) is given in Panel B. Note both the shape and associated values of the curves in Panel B. At the highest M value the inflexion point in the curve occurs at ~1000 g m^{-2} and year one. Decreasing M to 0.62 moves the inflexion to year 2 at ~1277 g m^{-2}. As M is decreased to 0.58 the inflexion point remains at year 2 as the maximum shell density increases to ~ 1560 g m^{-2}. The lower M values provide standing stocks of shell that are approximations for a number of the MD reefs in Figures 11, while a M value of 0.66 provides an approximation for the Great Wicomico and Piankatank Rivers in VA in Figure 12. The purpose of Panels C and D in Figure 14 is to dissect the standing stock

value of Panel B into annual shell Production (Panel C) and Loss (Panel D) rates. The relevant estimators are:

Production = # surviving oysters * increase in shell weight where interval (t_1-t_0) = one year
Shell loss = # oysters lost to mortality * shell weight at beginning of interval (one year)
Both have units of g shell m^{-2} y^{-1}

Figure 14. Simulations based on Figures 11 and 12. A: survival as a declining function wherein annual mortality, M, is a proportional value between 0.0 (no mortality) and 1.0 (all died). M values are consistent color coded among panels between 0.58 and 0.72. Survival is (1-M). B: standing stock of shell (g m^{-2}). C: annual shell Production (g $m^{-2}y^{-1}$). D: annual shell Loss (g $m^{-2}y^{-1}$). See text for additional details.

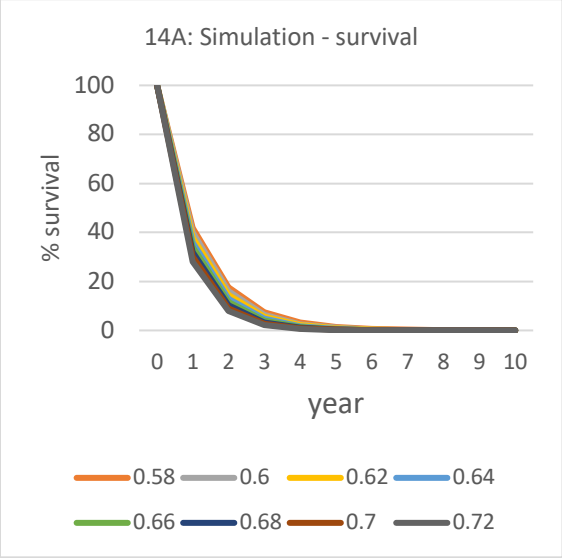

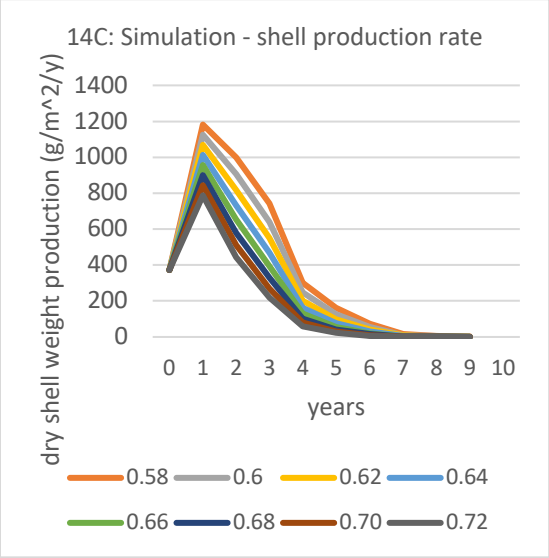

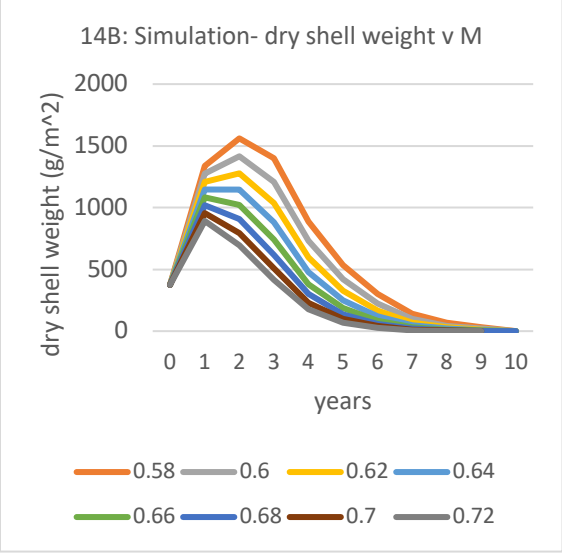

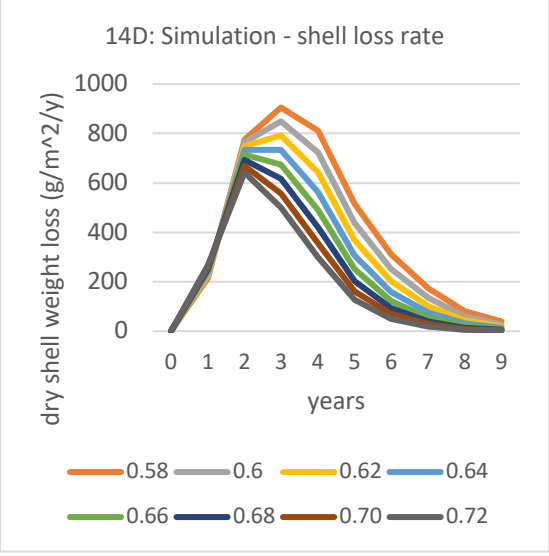

What is immediately evident from these plots is the dynamic nature of the shell pool. For example, even though shell standing stock in year two at M=0.60 is 1415 g m^{-2} the production for that year is 906 g m^{-2} and loss is 765 g m^{-2}. For the slightly higher M=0.66 shell standing stock is 1023 g m^{-2} and the production is 654 g m^{-2} and loss is 715 g m^{-2}. At the highest rate of M=0.72 shell standing stock is 694 g m^{-2} and the production is 444 g m^{-2} and loss is 499 g m^{-2}. These pools of shell have very high turnover rates. While the maximum shell standing stock values in Figure 14 are in the range 892 to 1561 g m^{-2} (M = 0.72 and 0.58 respectively) the shell production and loss (because the year class passes through completely) over the 10 year period for the year class varies between 1540 and 3488 g m^{-2} (M = 0.72-0.58 respectively).

How do these calculations influence our view of the stability of shell on extant reefs and the live shell to brown shell to loss rate relationship depicting in Figure 1? Table 8 provides a summary of live shell standing stock (LIVE, units dry shell, g m^{-2}), brown shell (BROWN, units dry shell, g m^{-2}), and live/brown ration (L/B) for VA areas 2006-2016 with all values rounded to nearest whole unit. This is a numerical summary of LIVE and BROWN data plotted in Figure 10 but in units of weight rather than volume. Of importance is the ratio L/B and the mean value for the eleven year period, underscored in the Table 8 presentation. These means vary between 0.13 and 0.32. Assuming that BROWN reflects a balanced input from LIVE and a loss to burial and taphonomy (see Figure 1) then the first approximation is that the L/B ratio represents a turnover or loss rate from the BROWN pool, that is between 13 and 32% of the pool is replaced annually. In fact this is wrong because the L/B ratio underestimates the input from the LIVE pool as illustrated by the plots in Figure 14 and the mortality rate dependent values given in the prior paragraph. In the range of mortality rates (M = 0.58-0.72) examined shell production exceeds peak standing stock by a factor of ~2.23 through 1.72 (3488/1561 = 2.23 at M = 0.58 through 1540/892 = 1.72 at M = 0.72). Taking an intermediate value of 2.0 from this range indicates that the turnover rate in the BROWN pool is between 26 and 64% annually. This range encompasses and reinforces the half-life estimates of Powell and Klinck (2007), and supports the general guideline implemented in VMRC Oyster Replenishment of shell planting every three years to approximately double standing shell stock on managed reefs.

I have thus summarized VA data. Can similar calculations be made for MD survey brown shell density on a per unit area basis? Swept area estimates of brown shell per unit area in MD surveys were generated from tow length, dredge width and bushel collected values. These were then converted to shell dry weight per unit area values using the following relationships:

I MD bushel = 2810 cu in = 45.9L,
1L wet shell = 597 g wet weight (Mann et al 2009a, 2009b), and
dry shell weight (g) = 0.93* wet shell (g) (r^2 = 0.99, n = 300 based on haphazard samples from 2013 MD condition sample oysters).

The conversion of wet shell volume to wet weight may appear illogical in that this gives wet shell a specific gravity of 0.597, less than that of water! This value is generated from loosely packed shell volume in collections made on the VA survey and reflects the fact that most of the volume in a bushel of oyster shell is space between the shells – we are weighing air. Hence the reason for the apparent nonsensical value. This "open shell" value is important in that when I return to a discussion of the disparity between extant and evolutionary based rates of shell production I use it as a basis for shell content in underlying shell/mud reef structure.

Table 8. Summary of live shell standing stock (LIVE, units dry shell, g m^{-2}), brown shell (BROWN, units dry shell, g m^{-2}), and live/brown ration (L/B) for VA areas 2006-2016. All values rounded to nearest whole unit. Mean values for each region are underscored.

	Tangier			*Pocomoke*			*Rappahannock 1-5*			*Rappahannock 6*		
	LIVE	BROWN	L/B	LIVE	BROWN	L/B	LIVE	BROWN	L/B	LIVE	BROWN	L/B
2006	278	3595	0.08	272	5341	0.05	285	3376	0.08	54	2747	0.02
2007	668	3985	0.17	807	4003	0.20	427	3158	0.14	176	2215	0.08
2008	957	4861	0.20	967	4649	0.21	565	3496	0.16	627	2426	0.26
2009	719	3789	0.19	544	3634	0.15	608	3188	0.19	486	2418	0.20
2010	633	3477	0.18	427	2538	0.17	553	3856	0.14	142	2841	0.05
2011	826	4445	0.19	1149	4905	0.23	557	3310	0.17	157	2504	0.06
2012	848	4029	0.21	1707	3979	0.43	1258	4169	0.30	417	2057	0.20
2013	666	3452	0.19	994	3415	0.29	990	3344	0.30	236	2542	0.09
2014	762	3878	0.20	779	2719	0.29	1047	3326	0.31	198	1793	0.11
2015	473	3646	0.13	157	2875	0.05	932	3904	0.24	459	2702	0.17
2016	775	3771	0.21	242	5429	0.04	1200	4237	0.28	607	2581	0.24
			0.18			**0.19**			0.21			**0.13**

	Great Wicomico			*Piankatank*			*York Mobjack*		
	LIVE	BROWN	L/B	LIVE	BROWN	L/B	LIVE	BROWN	L/B
2006	348	4211	0.08	278	3744	0.07	41	3282	0.01
2007	2061	5191	0.40	764	3347	0.23	621	5207	0.12
2008	1815	4902	0.37	868	3339	0.26	1444	5258	0.27
2009	1317	3943	0.33	951	3644	0.26	533	2594	0.21
2010	794	3643	0.22	993	4550	0.22	209	3818	0.05
2011	1354	7179	0.19	2390	5615	0.43	429	4070	0.11
2012	1275	6344	0.20	2101	6422	0.33	648	3040	0.21
2013	2563	6926	0.37	1610	4502	0.36	915	3392	0.27
2014	2203	5688	0.39	1903	4603	0.41	841	3531	0.24
2015	1537	4878	0.32	1812	4071	0.45	794	3392	0.23
2016	1961	5806	0.34	2082	4380	0.48	1320	4977	0.27
			0.29			**0.32**			**0.18**

	Lower James River			*Upper James River*			*Middle James River*		
	LIVE	BROWN	L/B	LIVE	BROWN	L/B	LIVE	BROWN	L/B
2006	158	1455	0.11	1960	7161	0.27	544	2422	0.22
2007	236	1672	0.14	1534	7609	0.20	568	2478	0.23
2008	223	2387	0.09	1644	7620	0.22	473	2288	0.21
2009	217	2037	0.11	2008	7296	0.28	586	2709	0.22
2010	221	3960	0.06	2243	7713	0.29	749	2972	0.25
2011	419	3885	0.11	2937	8504	0.35	914	2884	0.32
2012	352	2617	0.13	2092	7903	0.26	729	2702	0.27
2013	539	3149	0.17	1755	8213	0.21	651	2644	0.25
2014	617	2167	0.28	2095	7419	0.28	804	2506	0.32
2015	716	3212	0.22	2184	7950	0.27	672	2148	0.31
2016	1493	5049	0.30	2234	6937	0.32	837	2541	0.33
			0.16			**0.27**			**0.27**

Applying these conversions to the shell weights per unit area results across the entire swath of MD reefs sampled results in brown shell estimates that are comparable to or more often less than that of the live shell per unit area. Unlike the VA data as reported in Table 8, the MD relationship is variable and inconsistent both within and among reef sites. This appears illogical until the data are considered in the context of how a dredge functions. Unlike the patent tong that samples through the layers of the reef structure the dredge simply scrapes the upper surface. Thus, it is expected to most representatively sample the surface layer, and do so with decreasing efficiency with increasing depth into and hardness of the reef structure. As the underlying structure hardens penetration is reduced and the brown shell layer is under-sampled relative to the live oysters precluding an examination of the quantitative relationship between the two and forcing the focus of discussion on simple turnover rates of shell in the live portion alone. I re-emphasize, the MD dredge survey was never designed with the current examination in mind.

This rapid throughput of shell is important because the range of values described above will be employed later in this text in a simulation (Oyster_Mortality_Playbook in an Appendix) to compare current shell production and loss rates with that expected in fossil or pre-colonial demographics free of anthropogenic activity. The term anthropogenic is intentional to include not just harvest but all watershed and in river activities that collectively and cumulatively have impact on Bay oyster populations.

Evolutionary targets for oyster shell production and the disparity with observed values in extant reefs

The genus *Crassostrea* and its predecessors have been present in the fossil record for approximately 50 million years. Oysters evolved to be long-lived species whose survival is based on a life history strategy that employs enormous fecundity (see the final footnote on fecundity in extant populations surveyed for this study), coordinated spawning in aggregations of fecund adults, dispersal to many possible sites of recruitment (with associated staggering proportional losses to mortality in suboptimal environments), recruitment to reef systems that offer spatial refuge to early post recruit sizes, rapid growth to refuge size in these complex environments, and, very importantly, longevity in this size refuge for many years before succumbing to old age. In the absence of reefs oysters have effectively no habitat into which they can recruit. Maintenance of underlying reef structure is central to perpetuation of oyster populations (Mann and Powell 2007). Mann et al (2009a) pose the question "can the proposed population dynamics sustain an accretion rate commensurate with maximum sea level rise in the past 50 million year period?" What sea level rise values should we consider? The early Tertiary (30-60 MYA) may have experienced much less rapid sea level rises and falls than the glaciated late Tertiary (30 MYA – 1.8 MYA) and Quaternary (1.8 MYA to present; Vail and Mitchum, 1979; Pitman, 1978 in Kennett, 1982). Rates of sea level rise were higher in the early Holocene transgression (7,000 to 17,000 years ago) at 8 mm y^{-1} (Kennett, 1982, based on Curray, 1965; Milliman and Emery, 1968). The most rapid phase of the Holocene transgression was at 7,000-10,000 years ago with a rate of 10 mm y^{-1} (Kennett, 1982). The Chesapeake estuary experienced a relatively rapid transition from fresh to brackish water conditions between 7,400 and 8,200 years ago commensurate with sea level rise and/or the crossing of hydrographic or topographic barriers (Bratton et al., 2003). Landward intrusion of saltwater is marked by fossil oyster beds in the northern Chesapeake Bay and upstream areas of the Potomac River with subsequent oceanward retreat beginning about 6,000 years ago as rates of sea level rise decreased and the headwaters of the estuaries began to fill with sediment (Bratton et al., 2003). Thus the evolutionary target for oysters is in the region of 10mm y^{-1} plus an allowance for taphonomic loss and burial at 13-32% (or arguably twice that value - see above). Shell production rate to maintain equilibrium with sea level rise of 10 mm y^{-1} is estimated, assuming a conservative 30% loss y^{-1} to degradation processes, to be 13 mm y^{-1} or 13 L m^{-2} y^{-1} (one L covers one square meter to a depth of one mm) or 7,217 g m^{-2} y^{-1} dry shell. This conservative estimate is approximately five times higher than the maximum production rate in the third panel of Figure 14, and the disparity increases should a higher turnover rate in the brown shell pool be invoked.

How do extant shell production values compare with required values of accretion for reef stability in the face of current sea level rise? A brief summary from Mann et al (2009a) is appropriate. Current relative sea level rise, including both sea level rise and land subsidence, may be as high as 4.5 mm/y depending on location within the Bay. For oysters this may be compounded by location dependent sedimentation, which can be comparable or higher in rate than sea level rise (see Hobbs et al 1990, also note historical perspective Bratton et al., 2003). In this section of the report I examine longevity and mortality rate in oysters and how the truncation of life span in extant populations has impact on the ability of managers to rebuild current resources. We know from abundant fossil oysters that longevity and large terminal size is part of the oyster evolutionary ambit. I add another proverbial twist to this conversation. Oysters have been widely described as exhibitors of type 3 mortality curves – that is a declining exponential mortality. In fact I use this function in generating data in both Mann et al (2009a) and in Figure 14 of this report. But I also argue that this single declining exponential is wrong when considering an extended life span as for fossil oysters. Indeed I proffered the argument for age dependent mortality rates seven years ago (Mann et al 2012), and that the mid-life of oysters, like that of *Homo sapiens*, is characterized by low mortality rates. Associated with this mid-life period is continual production of shell, and only when mortality rates increase again later in the life span is this shell added to the underlying reef structure where its fate and loss dynamics are controlled by burial and taphonomy. This period of extended mid-life growth and production is absent in extant populations – they die before attaining this refuge status (and thus a single declining exponential is appropriate for Figure 14). This truncated longevity insures that shell addition rates to the underlying reefs will decrease and compromise reef structure – I will demonstrate this later in the report. In the following text I defend my argument for a complex mortality curve and then proceed to examine the discrepancy between single and complex mortality curves in the current management challenge.

What evidence exists to support the opinion of a complex mortality curve? I have, as illustrated, extensive demographic data from stock surveys in oysters in both MD and VA. Can this be compared with pre-colonial periods when oysters were effectively undisturbed? Are there other sources of comparable? The answer is in two places – the fossil record (Lockwood and Mann 2019, in review and unpublished data from my lab) and in a rare population of invading oysters in a location where parasites, diseases and predation (including harvest) are absent (Walles et al 2015). These I use to develop this section of the report and address the complex mortality question.

The current Chesapeake Bay was gradually inundated in the late Holocene by rising sea level; however, the Bay geological record also contains fossil reef structures from prior high stanzas. The first data set employed in this section was collected from a reef in the central section of the Piankatank River, VA. This has been described in Lockwood and Mann (2019, in review), and for the current purpose the demographic data in Figure 1 of that contribution is reproduced here as Figure 15 of the current report. Of particular note is the consistent representation of size classes up to and including ~130mm SL (Lockwood and Mann, Fig 1*a*). Fitting a curve to the companion Fig 1*b* of Lockwood and Mann gives the descriptor $SL = 44.18x^{0.46}$, $r^2 = 0.72$, n = 108, where x is age (y). Applying the length-age relationship to Fig 1a of Lockwood and Mann illustrates that the period from ~60 through 130mm SL corresponds to 2 through ~11 years of age. As age increases above 11y (>130mmSL) representation in the demographic decreases. The suggestion here is a period of low mortality between ~2 and 11 years of age with increasing mortality thereafter with few oysters surviving above 20y. Note that a limitation with fossil data is probable under representation in the smallest (youngest) size (age) ranges simply because valves disarticulate quickly and are easily broken and degraded because they are so thin – but this does not discount the low mortality with mid-life argument.

The second fossil data set is for oyster shell collected on the inner continental shelf south of Long Island by a commercial hydraulic clam dredge in 2017 in ~90 feet depth. This deposit is probably in excess of 10,000y old, but no carbon dating has been pursued. The dating is relatively unimportant because this deposit, like the Piankatank fossil deposit, represents an undisturbed reef system. The Long Island collection is a demographic of 46 oysters that, when overlaid on the Piankatank River data (see Figure 16)

from Lockwood and Mann, provides comparable age at length and, again, good representation in the 60-160 mm SL and 4-8 y ages ranges. The demographic is again suggestive of modest mortality in this size and age range.

Figure 15. Figure 1 of Lockwood and Mann (2019, in review). Length frequency *(a)* and age at length *(b)* of Pleistocene oyster shells from the Piankatank River VA and modern shells from the James River VA.

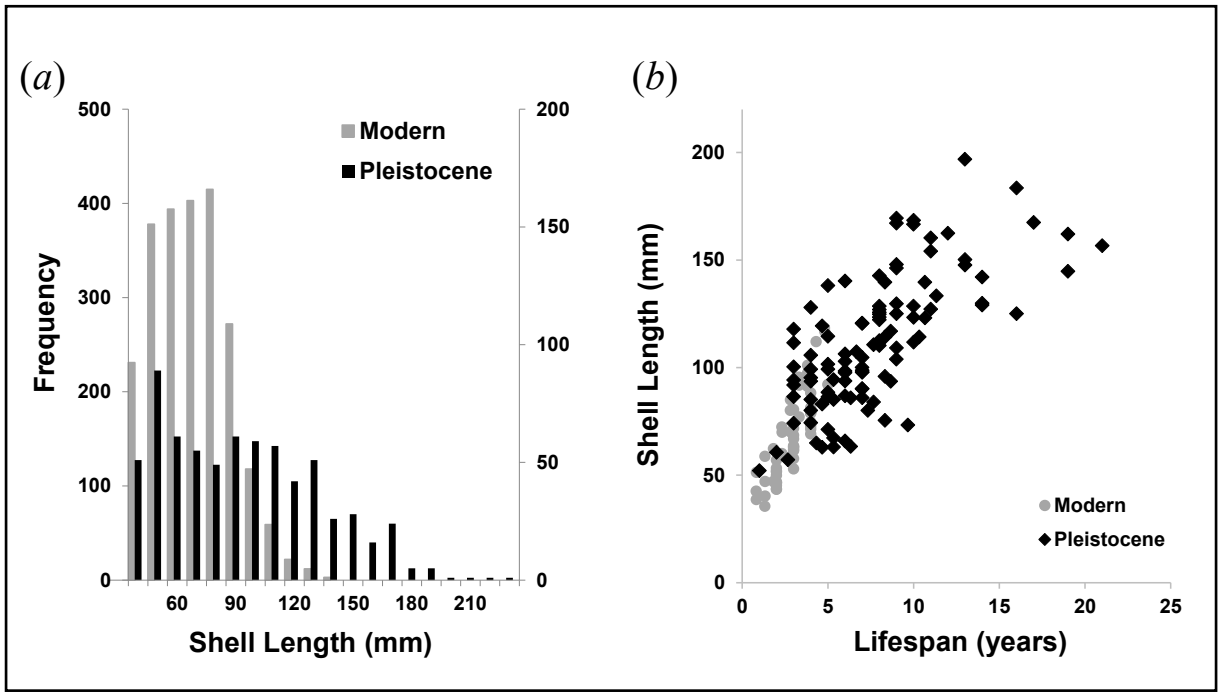

Figure 16. Length at age for fossil oyster shells: combined data from Piankatank River collection (blue, from Lockwood and Mann in Figure 15) and offshore New York (orange). See text for additional details.

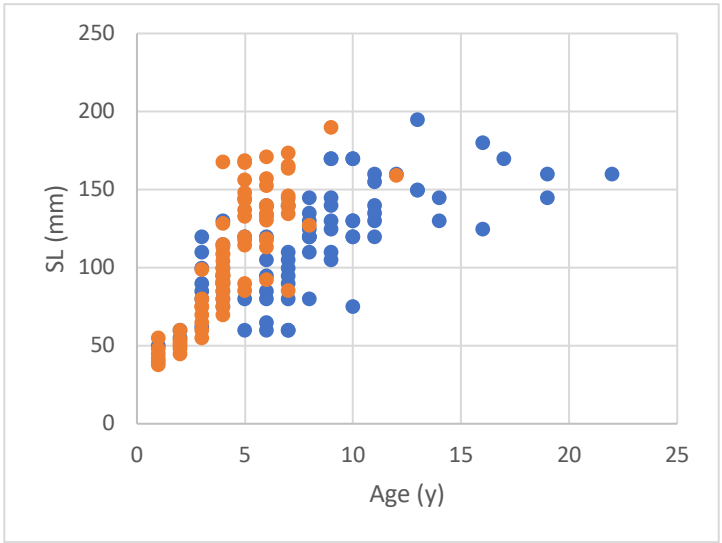

The final data set comes from an invading population of oysters, in this instance *Crassostrea gigas,* in the Netherlands Oosterschelde as described by Walles et al (2015). Length frequency distributions from three sites with very substantial n values again illustrate a period of high early life mortality through 30-50mm SL followed by a period of 5 or more years when the demographic suggests effectively no mortality, and an increased mortality rate through terminal sizes at >200mm SL. These are rapidly accreting reefs, see Walles et al (2015), and underscore the importance of many year classes in the live portion of the complex to reef persistence.

Walles et al (2015) provide a Weibull frequency distribution for their data, effectively a type 3 declining exponential. As noted earlier, Mann et al (2012), Mann et al (2019) and Lockwood and Mann (2019, in press) stated that the declining exponential was inappropriate and should be replaced with a minimally three component curve. Such a curve would have a steep initial decline, a mid-section of low mortality, and a terminal section of high mortality. The argument is illustrated in both a reconsideration of Figure 5 from Walles et al (2015), modified and presented as Figure 17 in this report, and the age demographic plots from Walles et al (2015) reproduced here as Figure 18 of this report. In Figure 17 note the position of values below (age 2) and above (age 5) the fitted curve consistent with the proffered three part descriptor, the broken line in Figure 17, as an alternative to the fitted Weibull distribution.

Figure 17. A proposed revision of Figure 5 from Walles et al (2015). The original Weibull distribution fit ($\lambda = 1$, $\kappa = 0.6$) is the solid line fitted to survivorship data (mean + s.e.) of three oyster populations (Viane, St. Annaland and Kats) in the Oosterschelde estuary, Netherlands (raw data in Figure 18). The proposed revision of the mortality curve is the broken line and incorporates three distinct mortality rates over the life expectancy.

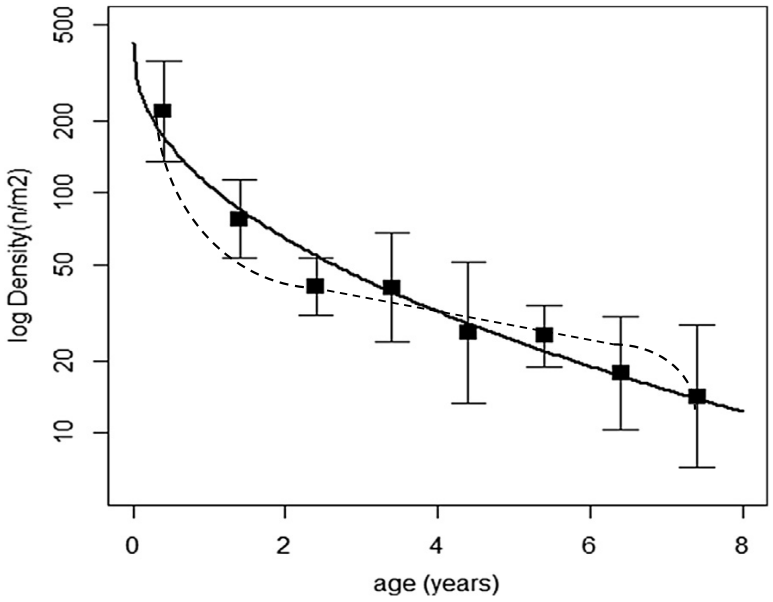

Figure 18. Length frequency distribution of oysters, *Crassostrea gigas* , pooled in 5 mm sizes bins, collected in 0.25 m^2 quadrants (n = 10) on three intertidal oyster reefs in the Oosterschelde estuary (The Netherlands): Viane, sampled November 1st 2011 (n = 2640); St. Annaland, sampled February 9th 2012 (n = 1341); Kats, sampled February 7th 2012 (n = 990). Year classes are separated by dashed lines. The arrows indicate the mean shell length for each year class. Source: Walles et al (2015)

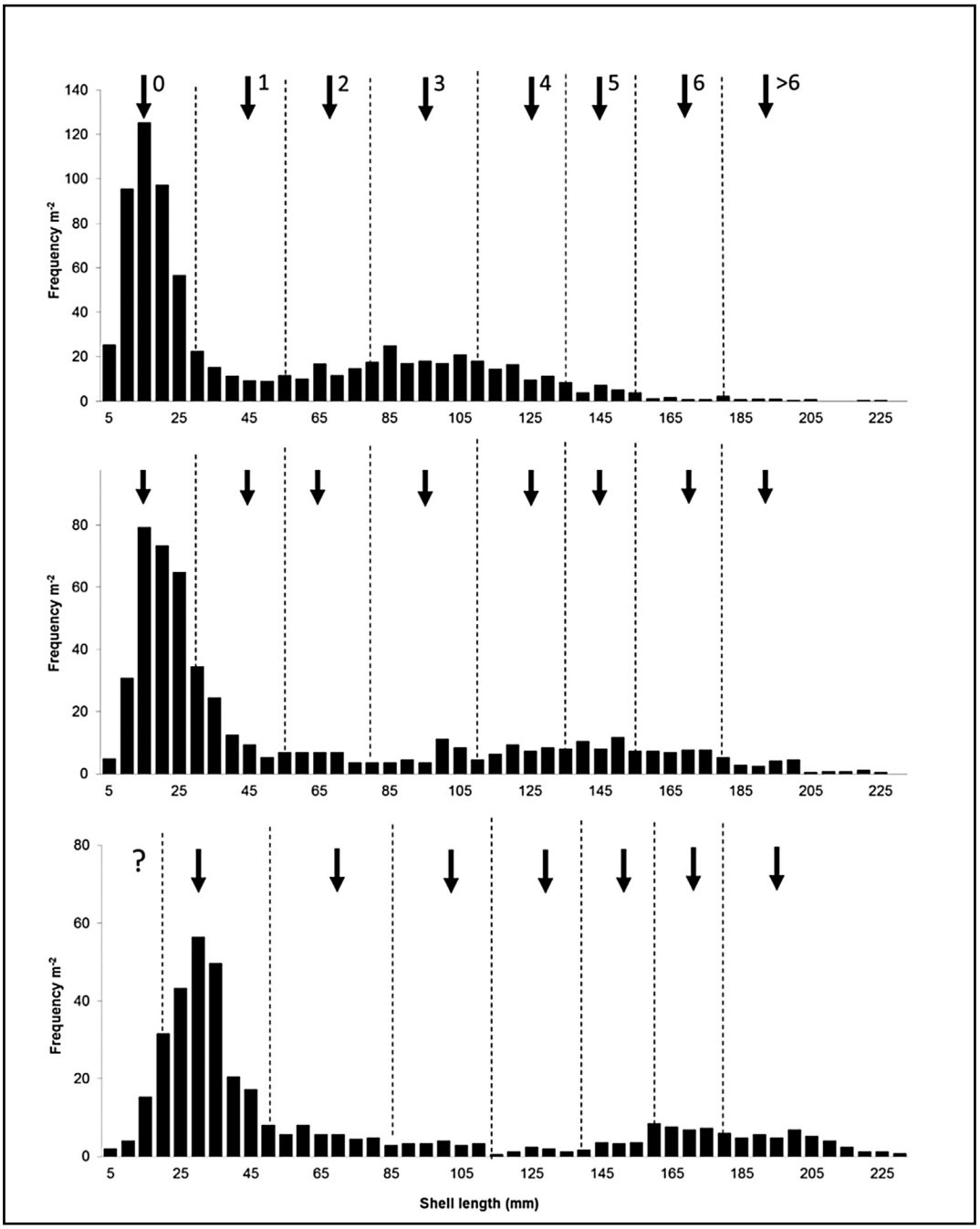

So the argument for a three part mortality curve is all well and good, but I need actual rates to provide estimators of shell production and loss in pre-colonial, undisturbed reef systems to compare to extant

systems described herein. For example purposes I propose a reef with a year class of oysters recruited at a density of 100 individuals per square meter as Young of the Year (YOY = spat), as used in Figure 14 for the simulation of VA oyster shell production and loss rates. To this I apply a 3 part mortality sequence with an initial high rate, a subsequent mid-life low rate, and a final high rate. These rates are reported in Table 9 and a sequence of accompanying results given in both Table 9 and Figure 19. The intent with this exercise is to replicate the demographic in Figure 15 and examine sensitivity of output to varying M. The early part of this fit can be achieved by employing a cumulative mortality for the YOY through 2 year old range taken as a mean value from 9 years of collections from the Piankatank River, VA (2006-2008, 2010, and 2012-2016) of 58%. Thus 42% survive to age 2, or a proportional annual loss of M = 0.35. This value is used in sequence #1 in Table 8 and Figure 19. A mid-life period M2 (3-11 y) with increasing values from 0.05 to 0.12, is followed by a later term M4 (12-20y) of 0.4. A challenge when fitting a sequence to the Lockwood and Mann data is that the smaller oysters in this demographic are underestimated because they are more easily broken and degraded in the taphonomic sequence. If they are underestimated then the initial value of M in sequence #1 is too low, and thus sequence #2 replicates #1 but with a higher value of M1 at 0.55. The longevity of the M2 period in the protocol is set by the earlier age interpretation of the Lockwood and Mann plot, but a third sequence is added using a shorted M2 period of years 3 through 8, based on the data of Walles et al (2015) in Figure 18. For comparison the data in Figure14, the generic description of extant populations with a single M rate throughout a 0-9 y period is added to the table. Sequences #1 through #3 use the fossil age at length curve of Figure 1B of Lockwood and Mann (see Figure 15 of this report) whereas the Figure 14 data set use the composite MD age at length curve (see page 21).

Figure 19 portrays a selection of subsets in sequences #1 through #3 as descending panels of component figures, with each descending line corresponding to sequences #1 through #3 respectively of Table 8[1]. The M1/M2/M3 progressions are given in the footer labels of each of the three upper panels, these corresponding to sequences #1 through #3 respectively of Table 8. The upper panels are survival. Note the substantial mortality in years 0-2. Sequences #2 and #3 have, by year 2, comparable losses to that in Figure 14. The M2 period in all plots show relatively little additional cumulative loss before a transition to notable final losses in the M3 mortality period. The second panel in each descending line illustrates shell dry weight, effective shell standing stock (g m^{-2}) over the course of the 20 year examination. While the patterns of increase and decrease with time are similar for the three numbered sequences note the scale of the values, also that plots for sequence #1 have ordinates with twice the maximum value of ordinates for sequences #2 and #3. Under sequence #1 a gradual rise in standing stock is observed through year 11 with maximal values varying from 4906 g m^{-2} at M1/M2/M3 of 0.35/0.12/0.4 to ~ 9,770 g m^{-2} at M1/M2/M3 of 0.35/0.0.05/0.4. An exponential decline occurs thereafter in all mortality options to zero at ~20 y of age. The comparable high values for sequences #2 are 2351 g m^{-2} and 4683 g m^{-2} for M1/M2/M3 of 0.55/0.12/0.4 and 0.55/0.0.05/0.4, and for sequences #3 are 2242 g m^{-2} and 3548 g m^{-2} with the same M1/M2/M3 values but M2 reduced to a 5 y period from year 3 through year 8. Even in the most conservative of these options the maximum shell standing stock values exceed the maximum in Figure 14B by a factor of ~1.5x, with the high value in sequence #1 exceeding the maximum in Figure 14B by a factor of >6. Additionally, the standing stock in sequences #1 through #3 are maintained for a period of several years whereas in Figure 14 the maxima are decidedly a single year peak value. Note that each of the sequences in both Figures 14 and 19 are single year classes progressing through time. A multi-year consideration wherein each year is a new cohort demands that the values in sequences #1 through #3 would be overlaid and additive with effective standing stocks being many times the values displayed in Figure 19. By contrast the single peak standing values in Figure 14 produce, when considered as a multi-year sequence, maximal values that are only modestly higher than the high values in Figure 14B. I will return to this disparity later in the text. The contrast in shell standing stock descriptors of fossil reefs (Figure 19), even conservative descriptors, with extant reef systems (Figure14) is stark.

[1] This figure is generated by a EXCEL program named Oyster_mortality_playbook.xlxs. It is described in detail in an Appendix and provided for the reader to further explore data options.

Table 9. Shell production (g m^{-2} y^{-1}), shell loss (g m^{-2} y^{-1}), and filtration index (L/h) values associated with oyster populations of initial density 100 m^{-2} and subjected to various sequences of mortality. Sequence #1 is a three part mortality protocol with M1 (0-2y) of 0.35, M2 (3-11 y) increasing from 0.05 to 0.12, and M4 (12-20y) of 0.4. The fossil age at length curve of Figure 1B of Lockwood and Mann (see Figure 15 of this report) is employed. Label 1 through 8 of sequence #1 correspond to 1 through 8 in Figure 19. Sequence #2 is a three part mortality protocol with M1 (0-2y) of 0.55, M2 (3-11 y) increasing from 0.05 to 0.12, and M4 (12-20y) of 0.4. The fossil growth curve of Lockwood and Mann is employed. Label 1 through 8 of sequence #1 correspond to 1 through 8 in Figure 19. Sequence #1 is a three part mortality protocol with M1 (0-2y) of 0.55, M2 (3-8 y) increasing from 0.05 to 0.12, and M4 (9-20y) of 0.4. The fossil growth curve of Lockwood and Mann is employed. Label 1 through 8 of sequence 1 correspond to 1 through 8 in Figure 19. The data of Figure 14 of this report is include for comparison purposes. A single value of M is employed for the 0-9 y period, with M increasing sequentially from 0.58-0.72. The composite MD age at length curve (see page 21) is employed. See text for additional discussion of Filtration Index.

	label	M1	period (y)	M2	period (y)	M3	period (y)	age v SL	shell prod (g/m^2)	shell loss (g/m^2)	filtration index (L/h)
sequence #1	1	0.35	0 thro 2	0.05	3 thro 11	0.4	12 thro 20	fossil	14286	14428	2417
	2	0.35	0 thro 2	0.06	3 thro 11	0.4	12 thro 20	fossil	13562	13704	2267
	3	0.35	0 thro 2	0.07	3 thro 11	0.4	12 thro 20	fossil	12881	13023	2127
	4	0.35	0 thro 2	0.08	3 thro 11	0.4	12 thro 20	fossil	12243	12385	1997
	5	0.35	0 thro 2	0.09	3 thro 11	0.4	12 thro 20	fossil	11643	11785	1875
	6	0.35	0 thro 2	0.1	3 thro 11	0.4	12 thro 20	fossil	11080	11222	1761
	7	0.35	0 thro 2	0.11	3 thro 11	0.4	12 thro 20	fossil	10552	10694	1655
	8	0.35	0 thro 2	0.12	3 thro 11	0.4	12 thro 20	fossil	10056	10198	1556
sequence #2	1	0.55	0 thro 2	0.05	3 thro 11	0.4	12 thro 20	fossil	7014	7113	1178
	2	0.55	0 thro 2	0.06	3 thro 11	0.4	12 thro 20	fossil	6667	6766	1106
	3	0.55	0 thro 2	0.07	3 thro 11	0.4	12 thro 20	fossil	6341	6440	1039
	4	0.55	0 thro 2	0.08	3 thro 11	0.4	12 thro 20	fossil	6035	6133	976
	5	0.55	0 thro 2	0.09	3 thro 11	0.4	12 thro 20	fossil	5748	5846	918
	6	0.55	0 thro 2	0.1	3 thro 11	0.4	12 thro 20	fossil	5478	5576	863
	7	0.55	0 thro 2	0.11	3 thro 11	0.4	12 thro 20	fossil	5225	5323	813
	8	0.55	0 thro 2	0.12	3 thro 11	0.4	12 thro 20	fossil	4987	5086	765
sequence #3	1	0.55	0 thro 2	0.05	3 thro 8	0.4	9 thro 20	fossil	**5353**	5452	782
	2	0.55	0 thro 2	0.06	3 thro 8	0.4	9 thro 20	fossil	**5168**	5267	749
	3	0.55	0 thro 2	0.07	3 thro 8	0.4	9 thro 20	fossil	**4991**	5089	718
	4	0.55	0 thro 2	0.08	3 thro 8	0.4	9 thro 20	fossil	**4821**	4919	687
	5	0.55	0 thro 2	0.09	3 thro 8	0.4	9 thro 20	fossil	**4657**	4756	659
	6	0.55	0 thro 2	0.1	3 thro 8	0.4	9 thro 20	fossil	**4501**	4599	631
	7	0.55	0 thro 2	0.11	3 thro 8	0.4	9 thro 20	fossil	**4351**	4449	605
	8	0.55	0 thro 2	0.12	3 thro 8	0.4	9 thro 20	fossil	**4207**	4305	580
Figure 14	1	0.58	0 thro 9					MD	3488	3488	218
	2	0.6	0 thro 9					MD	3122	3122	192
	3	0.62	0 thro 9					MD	2791	2791	169
	4	0.64	0 thro 9					MD	2490	2490	149
	5	0.66	0 thro 9					MD	2217	2217	131
	6	0.68	0 thro 9					MD	1970	1970	115
	7	0.7	0 thro 9					MD	1745	1745	100
	8	0.72	0 thro 9					MD	1541	1541	88

Figure 19. Time series of survival, live shell standing stock (g m^{-2}), shell production and shell loss (g m^{-2} y^{-1}) for an oyster population with an initial density of 100 m^{-2} with varying sequences of mortality over a 20 year period. Sequence #1 is a three part mortality protocol with M1 (0-2y) of 0.35, M2 (3-11 y) increasing from 0.05 to 0.12, and M4 (12-20y) of 0.4. The fossil age at length curve of Figure 1B of Lockwood and Mann (see Figure 15 of this report) is employed. Label 1 through 8 of plots describing live shell weight, shell production and shell loss correspond to mortality rate sequences in the footer of the top panels of each sequence. See Table 9 and text for additional details.

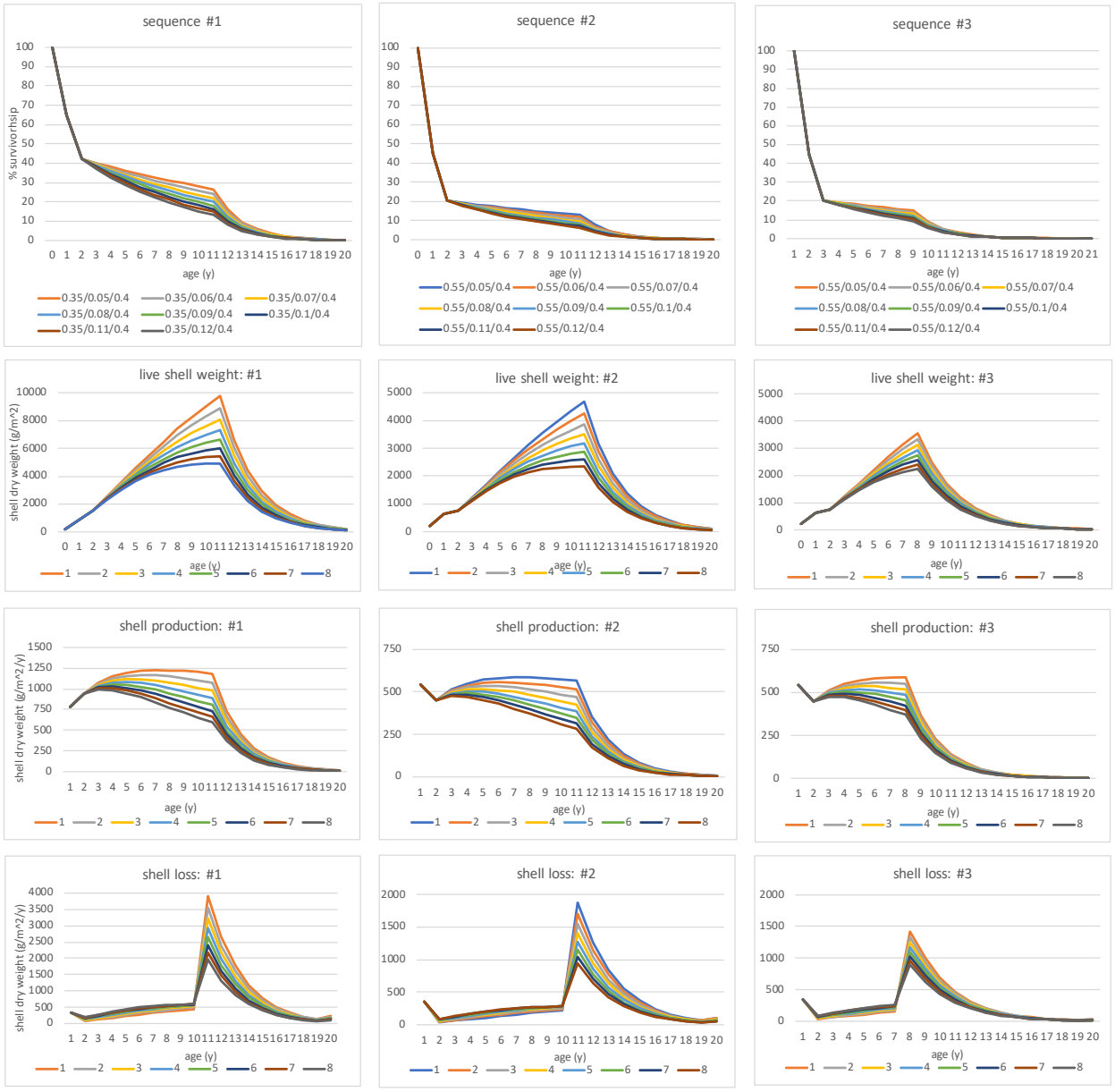

Proceeding to the third and fourth panels in each descending line in Figure 19, these partition the shell weights into production and loss components (g m^{-2} y^{-1}) for each year. As with Figure 14 the dynamics of the underlying contributions are masked by the general trends in the standing shell values. In all three

sequences there is notable stability in production rates until the M2 to M3 transition with exponential decay following that transition. The absolute production rates in sequence #1 are approximately double that of sequences #2 and #3, and maintained for approximately a decade – again contrast with the single year peak in Figure 14. The accompanying shell loss rates are low through the M2 to M3 transition, illustrating a noted spike at this transition as a large proportion of the large shells are added to the reef substrate in a period of just a few years. Again, when considering a series of cohorts progressing through the sequences in Figure 19, the expected pattern of shell provision to the reef substrate is that of large 8-12 year old oyster shells every year. What these plots do not include is a consideration of the eventual taphonomic loss and burial rates of these annually provided shells from mortality. I have alluded to more rapid loss of smaller shells earlier in this text – they are thinner and more easily broken providing greater surface area for biological and chemical degradation. What is missing is a critical rate measurement for loss rates with oyster size in the Bay ecosystem, indeed in any major estuary. Such data are needed to improve the current analysis and are critical in that the Bay ecosystem is replete with small rather than large oysters. An experimental approach is feasible, although there may exist an option to examine this small versus large rate debate in comparing demographics of live shell and brown shell where the time series between the two is coherent. A "loss" of smaller shells relative to larger shells in the brown shell would be driven by differing shell breakage/burial/dissolution rates.

The ninth and tenth columns of Table 9 are the cumulative values of annual shell production and shell loss in the plots in Figures 19 and 14 in units of g m^{-2} y^{-1}. The slight difference in the production and loss values for sequences #1 through #3 are the product of application of the Lockwood and Mann fossil age at length curve. This curve is fitted but not forced through zero. Thus an intercept at age 0.25 y (3 months) is equivalent to an SL of 23.4mm. This is loaded in to the EXCEL simulator that produces Figure 19 as the "zero' value for YOY and the YOY to age 1 interval is slightly smaller than the subsequent annual increments. By comparison the MD composite age at length relationship is better defined at YOY because the season of sampling is well known with respect to the recruitment to benthos period. This modest difference has little impact on the overall picture portrayed by the analysis. The range of production and loss values from Figure 14 are below all of the values for the sequence #1 through #3 options – the most conservative in sequence #3 exceeding the maximum from Figure 14 by a factor of 1.2 whereas the maximum value from sequence #1 exceeds the maximum from Figure 14 by a factor of 4. Again, the contrast in shell standing stock descriptors of fossil reefs with extant reef systems is stark.

The final column in Table 9 is a filtration index and provided for discussion because it is both easily generated in the Oyster_mortality_playbook.xlxs file using the data from Powell at el (1992), and relevant to the subject of Bay water column filtration and benthic -pelagic coupling so elegantly debated by Newell (1988). Powell provides a filtration rate estimator for oysters at 25^{o}C based on their dry meat weight (here DMW g). Using the SL v DMW relationship for the Piankatank River a separate line in Oyster_mortality_playbook.xlxs provides a standing stock DMW in parallel to the DSW shell values given throughout this report. For each year in the sequences in Table 9 filtration rate has been calculated based in the Powell et al relationship, then the values summed over the time frame of the simulation. These summed values are thus a relative index of filtration – they are not absolute values of volumes of water filtered. These indices provide relative estimates of filtration by the demographics portrayed as fossil reefs and representative extant reefs. Again, the lowest value of this index for the most conservative in sequence #3 exceeds the maximum from Figure 14 by a factor of 2.6 whereas the maximum value from sequence #1 exceeds the maximum from Figure 14 by a factor of 11. Yet again, the contrast in shell standing stock descriptors of fossil reefs with extant reef systems is stark.

The extensive data generated in support of Figures 11, 12, 14 and 19 provide valuable quantitative estimates of shell production on a unit area basis. Can we apply these to estimate both thickness of the shell layer on the reef and reef accretion? Ten liters of shell covers an area of one square meter to the depth of one centimeter. 1L wet shell = 597 g wet weight (Mann et al 2009a, 2009b), and dry shell weight (g) = 0.93*

wet shell (g). Thus 555 g of dry shell provide 1L of shell volume, and 10X this weight provides one centimeter depth when the air spaces included in the wet weight estimate from loosely packed shell are filled instead with sediment on the reef surface. The high standing stock values in Figure 14 range between 800 and ~1550 g m^{-2} or approximately 1.5 – 3.0 mm thickness, barely more than one to two shells thick when evenly spread. The maximal production rates are ~ 750-1200 g m^{-2} y^{-1}, or addition of, again 1.5-2.5 mm depth when evenly spread. In the upper part of the Bay this a just keeping pace with sea level rise, but probably not the combination of seal level rise and sedimentation. Nearer the Bay mouth these rates fall below that of relative sea level rise. The proverbial bottom line is that reefs are losing ground with the fight against sea level rise and sedimentation in the Bay – but we already know that because repletion is required to maintain them. The scenarios for fossil reefs in Figure 19 provide standing shell stocks of between ~2000 and 10,000 g m^{-2} of dry shell in living oyster – between 4mm and 2 cm of uniform live oyster biomass across the reef surface. This is continuous layer of living oysters, undoubtedly arranged not a planar residents but with hinge buried in the sediment and the mantle gap upwards. Fossil reef production rates vary in the 300-600 g m^{-2} y^{-1} for the entire M2 period in sequences #2 and #3, and double this in sequence #1. Thus while this 300-1200 g m^{-2} y^{-1} range of production in a single year is comparable to Figure 14, the persistence of the cohort in fossil reefs is for approximately a decade, meaning that at any one time there are up to ten cohorts each contributing shell in the 300-1200 g m^{-2} y^{-1} range. Taking a modest midway production value of 750 g m^{-2} y^{-1} for 10 cohorts in unison is 7500 g m^{-2} y^{-1} or approximately one centimeter of annual accretion spread evenly **after** accounting for losses as outlined on page 35. Given that for much of this accreting period the partner shell loss is at 25-50% of the production rate (Figure 19) then a **very conservative** estimate for accretion remains in excess of most sea level rise estimates over the past 50 million years, with highest sea level rise rates being within the range of accretion rates described by Figure 19.

In summary:

Extant reefs are losing the race with sea level rise and sedimentation; reefs represented in the fossil record had the race in hand. The disparity between the two is stark and unlikely to be reduced given the inability of oysters to survive to older ages in the current Bay ecosystem. This opinion is strongly supported by the current analysis. There is a fundamental challenge with longevity for Bay oysters and it cannot be blamed entirely on harvest or disease. A broader consideration of the Bay watershed and its input to the Bay should be carefully scrutinized. Truncated population structure reduces input of shell to the underlying reef structure such that the latter is not sustainable without continual shell repletion. Restoration to self-sustaining reef structures is unlikely, if not impossible, in extant oyster populations in the Bay.

Endnote: on the fecundity of oysters on extant reefs

The series of calculations and estimations that form the basis of this report also offered the opportunity to explore other features of the extant reef systems. Most are beyond the scope of this report, and indeed the subject of active analysis and research (for example the stock-recruit relationship in Bay oysters) and will result in reports and publications at a later date. None the less examination of fecundity in Bay oysters is worth of mention here. Truncation of life expectancy in oysters also limits reproductive capability. Oysters are protandric hermaphrodites, first maturing as males and transitioning to females with advancing age. A quantitative examination of this trait for Virginia oysters has been reported by Harding et al (2013). Using the demographic data reported earlier the whole population fecundity has been calculated for each of the nine VA areas reported above and are presented as cumulative values in the figure below. What is universally evident in these plots is how the lack of females >80mm SL curtails fecundity estimates. Stated simply, older and large oysters are needed to provide eggs if these systems are to increase both oyster populations and the underlying shell resource.

Figure 20. Cumulative fecundity (all size classes, egg m-2 y-1) for VA regions by year. All plots have the same axes with shell length on x axis and fecundity on ordinate. Note that ordinates are area specific in scale. All panels have the same color coding for years (e.g., 2009 is yellow throughout).

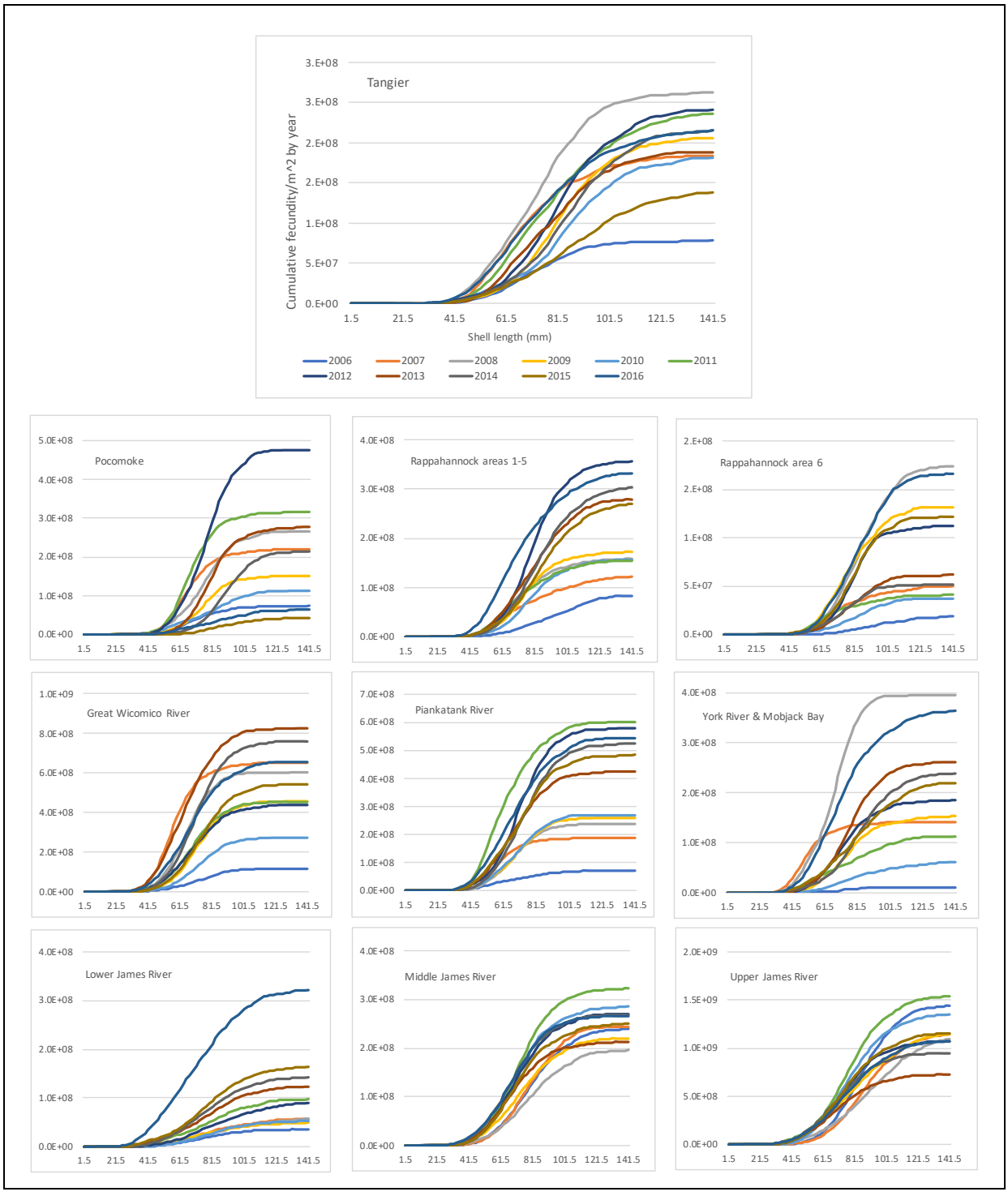

Literature cited

Bhattacharya, C. G. 1967. A simple method of resolution of a distribution into Gaussian components. Biometrics 23:115–135.

Bratton, J., S. Colman, E. Thieler, R. Seal. 2003. Birth of the modern Chesapeake estuary between 7.4 and 8.2 ka and implications for global sea level rise. Geo-Marine Letters 22, 188-197.

Bros, W. E., B. C. Cowell. 1987. A technique for optimizing sample size (replication). J. Exp. Mar. Biol. Ecol. 114:63–71.

Curray, J. 1965. Late Quaternary history, continental shelves of the United States. In: Wright, H. Jr., D. Frey. (Eds.), The Quaternary of the United States. Princeton University Press, Princeton, NJ, pp. 723-735.

Harding, J.M., E.N. Powell, R. Mann, M.J. Southworth 2013. Variations in Eastern oyster (*Crassostrea virginica*) sex ratios from three Virginia estuaries related to growth and mortality. Jour. Mar. Biol. Assoc. U.K. 93(2): 519-531.

Harding, J. M., M.J. Southworth, Mann, R., J. Wesson. 2012. Comparison of *Crassostrea virginica* Gmelin (Eastern Oyster) recruitment on constructed reefs and adjacent natural Oyster bars over decadal time scales. Northeastern Naturalist. 19(4): 627-646. DOI: http://dx.doi.org/10.1656/045.019.0407

Harding, J. M., R. Mann, M. Southworth, J. Wesson. 2010. Management of the Piankatank River, Virginia, in support of oyster (*Crassostrea virginica*, Gmelin 1791) fishery repletion. J. Shellfish Research 29(4): 1-22.

Hobbs, C. H., J. P. Halka, R. T. Kerhin, M. J. Carron. 1990. A 100-Year Sediment Budget for Chesapeake Bay. Special Reports in Applied Marine Science and Ocean Engineering (SRAMSOE) No. 307. Virginia Institute of Marine Science, College of William and Mary. https://doi.org/10.21220/V5RX6S

Kennett, J., 1982. Marine Geology. Prentice Hall, Englewood Cliffs, NJ. 813 pp.

Lockwood R., R. Mann. 2019 (in review). A conservation Paleobiological Perspective on Chesapeake Bay Oysters. Philosophical Transactions of the Royal Society B.

Mann, R., E. N. Powell. 2007. Why oyster restoration goals in the Chesapeake Bay are not and probably cannot be achieved. J. Shellfish Res., *26*, 905–917.

Mann, R., J. M. Harding, M. Southworth. 2009a. Reconstructing pre-colonial oyster demographics in the Chesapeake Bay, USA. Estuarine, Coastal and Shelf Science 85: 217-222

Mann, R., M. Southworth, J.M. Harding, J. Wesson. 2009b. Population studies of the native oyster *Crassostrea virginica* (Gmelin) in the James River, Virginia, USA. J. Shellfish Research. 28(2): 1-30.

Mann, R., B. Walles, K. Troost and T. Ysebaert. 2012 Abstract. So what should a natural mortality curve look like for oysters? National Shellfisheries Association AGM. Seattle, March 2012

Milliman, J.D., K.O. Emery. 1968. Sea levels during the past 35,000 years. Science 162, 1121-1123.

Newell, R.I.E. 1988. Ecological changes in Chesapeake Bay: Are they the result of overharvesting the American oyster, *Crassostrea virginica*? p. 536-546. in: M.P. Lynch and E.C. Krome (eds.), Understanding the Estuary: Advances in Chesapeake Bay Research. Chesapeake Research Consortium, Publication 129 CBP/TRS 24/88, Gloucester Point, Virginia.

Powell, E.N., E. E. Hofmann, J. M. Klinck, S. M. Ray. 1992. Modeling oyster populations. 1. A commentary on filtration rate. Is faster always better? J. Shellfish Res. 11(2): 387-389.
Powell, E. N., J. M. Klinck. 2007. Is oyster shell a sustainable estuarine resource? J. Shellfish Research. 26: 181–194.

Powell, E. N., J. M. Klinck, K. A. Ashton-Alcox, J. N. Kraeuter. 2009. Multiple stable reference points in oyster populations: biological relationships for the eastern oyster (*Crassostrea virginica*) in Delaware Bay. Fish. Bull., 107: 109–132.

Powell, E.N., R. Mann, K. A, Ashton-Alcox, Y. Kim, D. Bushek 2015. The Allometry of Oysters: Spatial and Temporal Variation in the Length-Biomass Relationships for *Crassostrea virginica*. J. Mar. Biol. Ass. UK. doi:10.1017/S0025315415000703. 18 pages.

Southworth, M., J. M. Harding, R. Mann, J. Wesson. 2010. Oyster (*Crassostrea virginica* Gmelin 1791) population dynamics on public reefs in the Great Wicomico River, Virginia, USA. J. Shellfish Research 29(2): 271-290.

Vail, P.R., R. M. Mitchum, Jr. 1979. Global cycles of relative changes of sea level from seismic stratigraphy. In: Watkins, J.S., L. Montadert, P.W. Dickerson, (Eds), Geological and Geophysical Investigations of Continental Margins. American Association of Petroleum Geologists Memoir 29, pp. 469-472.

Appendix: An introduction to Oyster_mortlity_playbook

This appendix describes an interactive simulator in EXCEL. An EXCEL file is appended to this report - Filename: Oyster_mortality_playbook.xlxs. The reader can follow the described sequence of actions that provide a final estimate of shell production and loss rates under reader defined conditions.

- Set that value in cell B10 for young of the year density (YOY = spat in # m^{-2}).
- Column A is the mortality rate (M) as a simple proportion of the density lost with each increment year. Thus a value of 0.1 is a loss of 10% of the oysters in one year. Using a single value of M to explain long lived individuals requires very low values for M throughout life – for examples see Mann et al (2009a).
- A single exponential decay curve and the demographic does not fit the above where many old oyster are represented. We need *minimally* a two part curve with initially higher M and lower M in later life to fit the observed data for undisturbed populations, or *better still* a three part curve where M increases again late in life.
- What is the best value for M1 to describe the initial period of high mortality? This is discussed in the report text. In this example I use an eight year mean for cumulative mortality from YOY to two years old (60mm) is 58%. Thus survival = 42%. Set M1 at 0.35 to reflect this survival rate. This is highlighted on row 14 of the example. Note this is a lower M value that is explored and fitted for the Figure 14 simulation, so higher M values can be explored, and indeed they are in this spreadsheet where the calculations are reported twice more in columns Y through AT and AW through BR.
- I explore a mix of M values and combinations throughout the life span, starting with M1 =0.35 for years 1 and 2 (values in red in B25 through D32), then reducing to M2 at year 3 onwards (values in blue, E40 through M47).
- I have set the value of M2 at 0.05 through 0.12 to find a match to the observed demographic in Lockwood and Mann (Figure 15, panel *a*). The reader can change the M2 value in cells A25-AW through BR32 as desired.
- I invoke M3 to reflect increased mortality in later years. In this instance a value of M3 = 0.4 results in mortality of the majority of oysters by age 18. Again, the reader can change values for M3 in cells A40-A47 as desired to explore end points.
- The simulator provides a mix of demographics from those that have many age classes represented to others with very few - and is thus a tool for exploration.

The above sequence provides a reasoned mortality rate and demographic descriptor for the fossil data in Figure 15 as described in the text in Table 9 and Figure 19.
The age at length "fossil" curve is that of Lockwood & Mann ($SL = 44.18x^{0.46}$, $r^2 = 0.72$, n = 108, where x is age (y)). Note that this is somewhat slower than the composite MD growth curve applied in Figure 14. Whether or not this may be the result of density dependent growth at the high fossil reef densities is open to debate. The SL versus biomass (DMW) and dry shell weight (DSW) allometric relationships are taken from current day Piankatank River oysters – these are based on high n values (n = 297 in both instances) but do require a large extrapolation (always a cause for concern) for the current exercise. This would be the case for any of the current allometric relationships given the absence of substantial numbers of large oysters in all extant populations. Thus:

$DMW = a*SL^b$ where a = 4E-05, b = 2.36 and r^2 =0.85
$DSW = a*SL^b$ where a = 2E-04, b = 2.95 and r^2 =0.92.

With these in place the reader now has the opportunity to explore how the growth and mortality functions interacts with the shell demographic on lines 129-136 of the EXCEL file. Consider, for example, how the standing stock of "living shell", shell production and loss rates varies with mortality rate. This creates a set

of plots in the center of the file page, note how the absolute values and distribution changes. These are values to compare with data in Figures 11 and 12. Equally important in terms of system dynamics is PRODUCTION of shell, shell loss to the underlying reef from the MORTALITY portion, and the PRODUCTION/LOSS RATIO (lines 154-163). As in Figure 14 of the report note that shell production can occur even when standing shell stock decreases. Note also how shell loss is concentrated in the years of transition from M2 to M3, when production/loss rations go from >>1 to <<1, that is when additions are large oyster shells with large contributions per individual shell.